

# Estimating Black Hole Masses in Quasars Using Broad Optical and UV Emission Lines

Paola Marziani and Jack Sulentic

*INAF, Osservatorio Astronomico di Padova, Italia & Instituto de Astrofísica de  
Andalucía, CSIC, España*

---

## Abstract

We review past work using broad emission lines as virial estimators of black hole masses in quasars. Basically one requires estimates of the emitting region radius and virial velocity dispersion to obtain black hole masses. The three major ways to estimate the broad-line emitting region (BLR) radius involve: (1) direct reverberation mapping, (2) derivation of BLR radius for larger samples using the radius-luminosity correlation derived from reverberation measures, and (3) estimates of BLR radius using the definition of the ionization parameter solved for BLR radius (photoionization method). At low redshift ( $z \lesssim 0.7$ ) FWHM  $H\beta$  serves as the most widely used estimator of virial velocity dispersion. FWHM  $H\beta$  can provide estimates for tens of thousands of quasars out to  $z \approx 3.8$  (IR spectroscopy beyond  $z \approx 1$ ). A new photoionization method also shows promise for providing many reasonable estimates of BLR radius via high S/N IR spectroscopy of the UV region 1300 – 2000 Å. FWHM  $MgII\lambda 2800$  can serve as a surrogate for FWHM  $H\beta$  in the range  $0.4 \lesssim z \lesssim 6.5$  while  $CIV\lambda 1549$  is affected by broadening due to non-virial motions and best avoided (i.e. there is no clear conversion factor between FWHM  $H\beta$  and FWHM  $CIV\lambda 1549$ ). Most quasars yield mass estimates in the range  $7 \lesssim \log M_{BH} \lesssim 9.7$ . There is no strong evidence for values above 10.0 and there may be evidence for a turnover in the maximum black hole mass near  $z \approx 5$ .

*Keywords:* black hole physics, active galactic nuclei, quasars, emission lines

---

## 1. Estimation of Black Hole Masses in Quasars: an Introduction

The existence of supermassive compact objects in galactic nuclei was proposed to solve the energy problem raised by the discovery of radio galaxies Hoyle and Fowler (1963). They estimated that the mass of such an object had to be of the order of  $10^8$  solar masses. Hoyle and Fowler (1963) showed that nuclear reactions were insufficient to provide the energy and that the energy source had to be gravitational collapse (see also Salpeter, 1964; Zel'Dovich and Novikov, 1965). The discovery of quasars (Greenstein and Schmidt, 1964) and of rapid optical variability (Smith and Hoeffeit, 1965) exacerbated the problem because, at their redshift distances, many quasars apparently involve sources emitting  $10^3$  times the luminosity of an  $L^*$  galaxy within a volume much less than a parsec of diameter. Estimation of the masses for these black holes is therefore at the center of quasar astrophysics and cosmology.

The black hole mass of quasars is a fundamental parameter that relates to the evolutionary stage of quasars and of the accretion processes occurring within them. An estimate of black hole mass ( $M_{\text{BH}}$ ) allows one to assess the role of gravitational forces in the dynamics of the region surrounding the black hole. The power output of quasars is directly proportional to  $M_{\text{BH}}$ . There is much debate over how the evolution of quasar energetic output might affect the development and structure of the host galaxy, as well as larger scale structure formation and, at very high redshifts, the re-ionization of the Universe (e.g., Fan, 2010).

Early estimates of  $M_{\text{BH}}$  were based on the apparent similarity of quasar spectra and their line widths. The size of the emitting region can be written as:

$$\Delta r = \left( \frac{3L_{\text{line}}}{4\pi f_{\text{f}} \epsilon_{\text{line}}} \right)^{\frac{1}{3}} \quad (1)$$

where  $L_{\text{line}}$  is the line (typically  $\text{H}\beta$ ) luminosity,  $f_{\text{f}}$  is the filling factor and  $\epsilon_{\text{line}}$  is the line emissivity. This expression was used to derive  $M_{\text{BH}}$  by considering the nucleus as a bound system and line broadening due to gas cloud motions (Dibai, 1977, 1984; Wandel and Yahil, 1985). It is interesting to point out that an analogous argument (coupled with the relatively short timescale of observed continuum variations) was used immediately after the discovery of quasars to suggest a small emitting region size and large mass.

The similarity of quasar spectra implies a roughly constant ionization parameter  $U$  or a constant product  $U$  times the electron density  $n_e$  (Baldwin and Netzer, 1978; Davidson and Netzer, 1979), where

$$U = \frac{\int_{\nu_0}^{+\infty} \frac{L_\nu}{h\nu} d\nu}{4\pi n_e c r^2}. \quad (2)$$

Here  $L_\nu$  is the specific luminosity per unit frequency,  $h$  is the Planck constant,  $\nu_0$  the Rydberg frequency,  $c$  the speed of light, and  $r$  can be interpreted as the distance between the central source of ionizing radiation and the line emitting region. So basically  $r_{\text{BLR}}$  is  $\propto L^{1/2}$  using rather order-of-magnitude considerations and the assumption of constant  $U$  pointing towards large masses increasing with source luminosity.

## 2. The Virial Assumption

The virial mass is defined as:

$$M_{\text{BH}} = f \frac{r \delta v_r^2}{G}, \quad (3)$$

where  $f$  is a factor dependent on geometry of the emitting region,  $r$  is the distance of line emitting gas from the central black hole,  $\delta v_r$  is the line broadening due to virial motions, and  $G$  is the gravitational constant. All methods based on broad optical and UV lines (e.g. photoionization, reverberation) come down to estimating the broad line region (BLR) distance from the central continuum source (hereafter indicated as the BLR radius  $r_{\text{BLR}}$ ) and combining it with a broad line width to derive  $M_{\text{BH}}$ .

The term “Keplerian” is used to indicate the particular case of a gravitationally bound system where the virial theorem applies. Kepler’s third law is appropriate when mass is mainly concentrated in a single body and the self-interaction gravitational potential of any remaining mass can be neglected; in the case of quasars,  $M_{\text{BH}} \gg$  mass of the line emitting gas (i.e., not unlike the solar system if solar and planetary masses are compared). Therefore, the terms virial and Keplerian will be used synonymously in the quasar context.

The fundamental question is whether the virial assumption is correct for the line being used. Evidence in support of virialization come from early velocity resolved reverberation mapping studies (Gaskell, 1988; Koratkar and Gaskell, 1989, 1991) that excluded outflow as the broadening source in at least low-ionization lines. Circumstantial evidence for virial motion involves emission

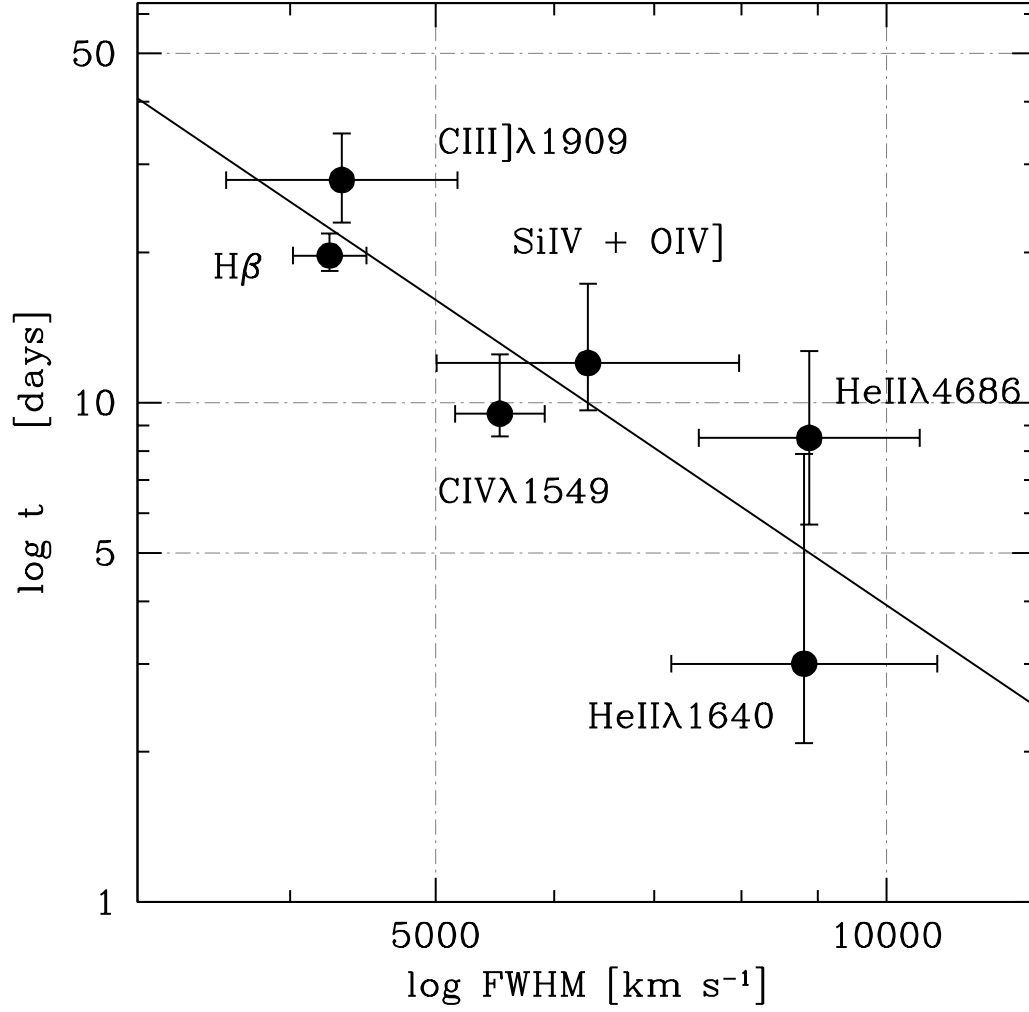


Figure 1: Test of virial broadening on several emission lines of NGC 5548. Adapted from Peterson and Wandel (1999). The line shows an unweighted least square fit.

line profiles of NLSy1-like sources which are relatively symmetric and smooth (Marziani et al., 2003a).

If the virial assumption is valid then the velocity field is Keplerian and line broadening should anti-correlate with the time lag of different lines (Peterson and Wandel, 1999; Peterson et al., 2004; Krolik, 2001). Sufficient data to test the width-distance relation are available for NGC 5548. Figure 1 shows a trend ( $r \propto \delta v_r^2$ ) consistent with dependence of time delay on line width. The delays of 6 emission lines (including the blend  $\text{OIV}] \lambda 1402 + \text{SiIV} \lambda 1397$ ) are plotted versus FWHM measures. Data come from the International AGN watch carried out in 1989. An unweighted least squares fit yields a slope of  $\alpha = 2.01 \pm 0.60$  which is consistent with the value expected for a Keplerian velocity field. A weighted least squares fit that takes into account errors on both axes yields a slope  $2.60 \pm 0.60$  indicating a strong increase in FWHM with decreasing distance.

Equation 3 is deceptively simple. Every term is problematic:

1. The geometric factor  $f$  allows us to convert an observed FWHM value into a virial velocity.  $f$  is poorly known because BLR geometry and effects of line-of-sight orientation are poorly known.
2. The distance  $r$  is highly uncertain because the BLR is not spatially resolved in any source.
3. The appropriateness of  $\delta v$  (virial broadening) rests on the assumption that lines are Doppler broadened reflecting motions of the emitting gas, and not by scattering (as considered by Mathis 1970; Kallman and Krolik 1986; Gaskell and Goosmann 2008). To estimate  $\delta v$  one must determine which line or line component (if any) is broadened by the motions of virialized gas. Line profile shifts relative to the quasar rest frame warn against indiscriminate use of line profile widths to estimate virial broadening.

### 3. The factor $f$

Our uncertainty about the geometric parameter likely represents a road-block to estimation of black hole masses more accurate than a factor of 3 – 5. If FWHM of a broad line is chosen as an estimator of  $\delta v_r$  and the velocity distribution is isotropic then the square of the velocity module is  $v^2 = 3v_r^2$  implying a geometric factor  $f \approx \sqrt{3}/2$ . In Eq. 3 our lack of knowledge about the geometry and dynamics of the BLR is concentrated in  $f$ . In other

words, an understanding of the dynamics and geometry of the BLR is directly related to the determination of  $M_{\text{BH}}$ . Considerable recent discussion and modeling have been directed towards estimating  $f$  and how it might depend on changing physical conditions (Collin et al., 2006; Onken et al., 2004; Netzer and Marziani, 2010). Radiation pressure forces and orientation effects make it possible that it is significantly ( $\times 3$  in Collin et al. 2006) and systematically different in Pop. A (FWHM  $\text{H}\beta \lesssim 4000 \text{ km s}^{-1}$ ) and Pop. B sources (FWHM  $\text{H}\beta \gtrsim 4000 \text{ km s}^{-1}$ ). Pop. A and B show striking differences in the  $\text{H}\beta$  and  $\text{C IV } \lambda 1549$  profiles and in several other properties (Sulentic et al., 2007). Although their interpretation in terms of BLR structure is not yet clear, further discussion in §6 will enlighten the importance of separating quasars into these two populations.

### 3.1. Dynamical effects

Given the strong radiation field to which gas is exposed in quasars it seems unlikely that gravity is the only important force. The relative balance of gravitational and radiation forces in a source of fixed  $M_{\text{BH}}$  points toward a role for Eddington ratio. The ratio between radiative and gravitational acceleration in an optically thick, Compton-thin, medium can be written as

$$r_a = \frac{a_{\text{rad}}}{a_{\text{grav}}} \approx 7.2 \frac{L_{\text{bol}}}{L_{\text{Edd}}} N_{\text{c},23}^{-1} \quad (4)$$

where  $L_{\text{bol}}$  and  $L_{\text{Edd}}$  are the bolometric and Eddington luminosities,  $N_{\text{c},23}$  is the hydrogen column density in units of  $10^{23} \text{ cm}^{-2}$ . If  $r_a > 1$  radiative acceleration dominates (cf. Netzer and Marziani, 2010; Marziani et al., 2010).

Very high column density clouds will be unaffected by radiative forces while lower column densities will be affected even at moderate Eddington ratios. A more refined dynamical treatment should consider the effects of radiative forces on a system of clouds moving in pressure balance with an external medium.

This approach indicates that the effect of radiation pressure significantly alters the equilibrium of a system of clouds: the emissivity weighted radius will increase as orbits become more elliptical and hence the cloud will spend a longer time at larger distances from the central continuum source. The value of  $f$  will therefore depend on Eddington ratio. At the same time the line will become narrower as radiation pressure increases. Fig. 2 shows

two  $H\beta$  profiles computed for confined clouds moving in pressure equilibrium with an external medium assuming a spherical distribution of orbits (Netzer and Marziani, 2010). Eddington ratio that has been set to  $L/L_{\text{Edd}}=0.05$  (at this low  $L/L_{\text{Edd}}$  the effect of radiative forces is small) and to  $L/L_{\text{Edd}}=0.5$  (appropriate for NLSy1-like Pop. A sources). The effect on FWHM and on the virial product  $r_{\text{BLR}}\text{FWHM}^2$  is rather modest, and the derived  $f$  increases from  $\approx 0.76$  to  $\approx 1.08$  along with  $L/L_{\text{Edd}}$ . How will these results affect single-epoch  $M_{\text{BH}}$  estimates in a large sample? The dependence of  $r_{\text{BLR}}$  on Eddington ratio will be a source of scatter in the  $r_{\text{BLR}}-L$  correlation. If this is taken into account we find an effect of less than a factor of 2 for  $M_{\text{BH}}$  estimates over 4dex in luminosity (Netzer and Marziani, 2010).

Previous work (Marconi et al., 2008, 2009) accounted for radiation pressure effects by adding an  $M_{\text{BH}}$  term proportional to the ratio  $L/N_c$  (where  $N_c$  was supposed to have a log-normal distribution with average  $\log N_c = 23$ ). In this case corrected  $M_{\text{BH}}$  can be a factor of even  $\gtrsim 10$  higher than values obtained using the virial formula (Gaskell, 1996). The implied masses of the most luminous quasars that would have been  $\gtrsim 10^{10} M_\odot$ , possibly reintroducing what we have called the “maximum mass problem” (Netzer, 2003): the most massive black holes at any redshift cannot exceed by a large factor the maximum mass of the (mostly quiescent) black holes at low  $z$ , around  $5 \cdot 10^9 M_\odot$  (the mass of the black hole in Messier 87; Macchetto et al. 1997). In other words, black holes with masses above  $5 \cdot 10^9 M_\odot$  should be extremely rare (Sulentic et al. 2006 and references therein). The Marconi et al. (2009) results are probably incorrect because they neglect the likelihood that the column density of bound clouds is dependent on Eddington ratio and hence on luminosity for a given mass.

### 3.2. *Estimating $f$ empirically: normalization*

The zone of gravitational influence for the black hole has been resolved in several nearby galaxies. The most reliable methods involve observation of  $H_2O$  masers (Miyoshi et al., 1995; Greene et al., 2010b; Kuo et al., 2011) or, at a second stance, space-based long-slit spectra of optical emission lines (e.g., Ferrarese et al., 1996; Macchetto et al., 1997; Barth et al., 2001; Capetti et al., 2005). Both methods spatially resolve the velocity field and yield a radial velocity “cusp” indicative of distances where the velocity field is

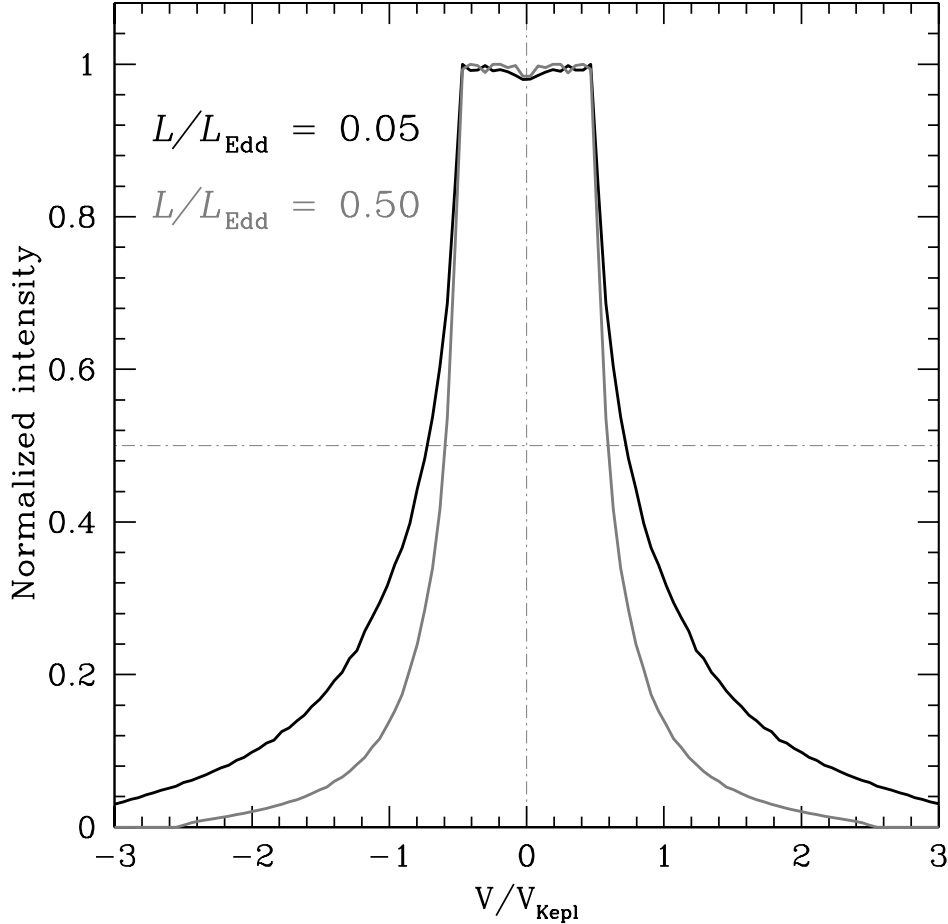


Figure 2: Effects of radiation pressure on line profiles computed for a spherical distribution of clouds in pressure equilibrium following Netzer and Marziani (2010). Model parameters are kept the same save for the Eddington ratio that has been increased by a factor 10, from  $L/L_{\text{Edd}} = 0.05$  to  $L/L_{\text{Edd}} = 0.5$ . The dot-dashed lines mark the rest-frame origin and the half maximum intensity level.

governed by gravity of the black hole. Mass values obtained from gas dynamics are considered less reliable since the line emitting gas might be more affected by non-circular motions (e.g., Barth et al., 2001; Shapiro et al., 2006).

Black hole masses computed from resolved velocity fields correlate with stellar velocity dispersion measures in the bulges of host galaxies (Ferrarese and Merritt, 2000; Gebhardt et al., 2000). The  $M_{\text{BH}} - \sigma_*$  correlation obtained for veloc-



ity resolved galaxies has been used to estimate  $f$  which can then be used for computation of quasar BH masses obtained from reverberation mapping derivations of  $r_{\text{BLR}}$ . One basically overlaps the  $M_{\text{BH}} - \sigma_*$  relations for non-active galaxies and AGN where  $\sigma_*$  has been estimated, usually from the IR Calcium triplet (Onken et al., 2004; Collin et al., 2006; Gültekin et al., 2009; Woo et al., 2010; Graham et al., 2011).

The derived  $f_\sigma \approx 5.5$  of Onken et al. (2004, where  $f_\sigma$  refers to the  $f$  value when the velocity dispersion is used as virial broadening estimator) was reputed a valid estimate but a recent study now suggests  $f_\sigma \approx 2.9$  (Graham et al., 2011), halving the  $M_{\text{BH}}$  values. Considering that the  $M_{\text{BH}} - \sigma_*$  relation for nearby galaxies shows significant scatter, results are subject to substantial uncertainty. In addition, there are two fundamental caveats:

1.  $M_{\text{BH}} - \sigma_*$  correlation of nearby galaxies could be a selection effect (Kormendy, 1993): only the most massive black holes can be resolved for a given bulge mass. The relation between  $M_{\text{BH}}$  and  $\sigma_*$  should be taken with special care in the lower  $M_{\text{BH}}$  range. This issue is farther discussed in §9.
2. It is unlikely that a single  $f$  value is valid.  $f$  appears to depend on the width of the  $\text{H}\beta$  line or, almost equivalently, on its shape. Collin et al. (2006) separated the reverberation sample in two populations: the Pop. A and B of Sulentic et al. (2000a) and Pop. 1 and 2 according to a profile shape criterion. This difference reflects different geometries that should also lead to different responses to continuum changes. This most interesting result of Collin et al. (2006) should be taken into account in any eventual attempt to derive  $f$ .

### 3.3. Orientation Effects

Orbits of BLR clouds are unlikely to be oriented randomly resulting in a strong dependence of  $M_{\text{BH}}$  on orientation. The  $f$  value derived by Collin et al. (2006) indicates that low-ionization line (LIL) emission in Pop. A sources may arise in a flattened configuration. Other lines of evidence suggesting a flattened gas distribution have been reported since the 1970s (they have been recently reviewed by Gaskell 2009b). Sources viewed at high inclination will then be measured with too small FWHM leading to systematic underestimation of  $M_{\text{BH}}$ .

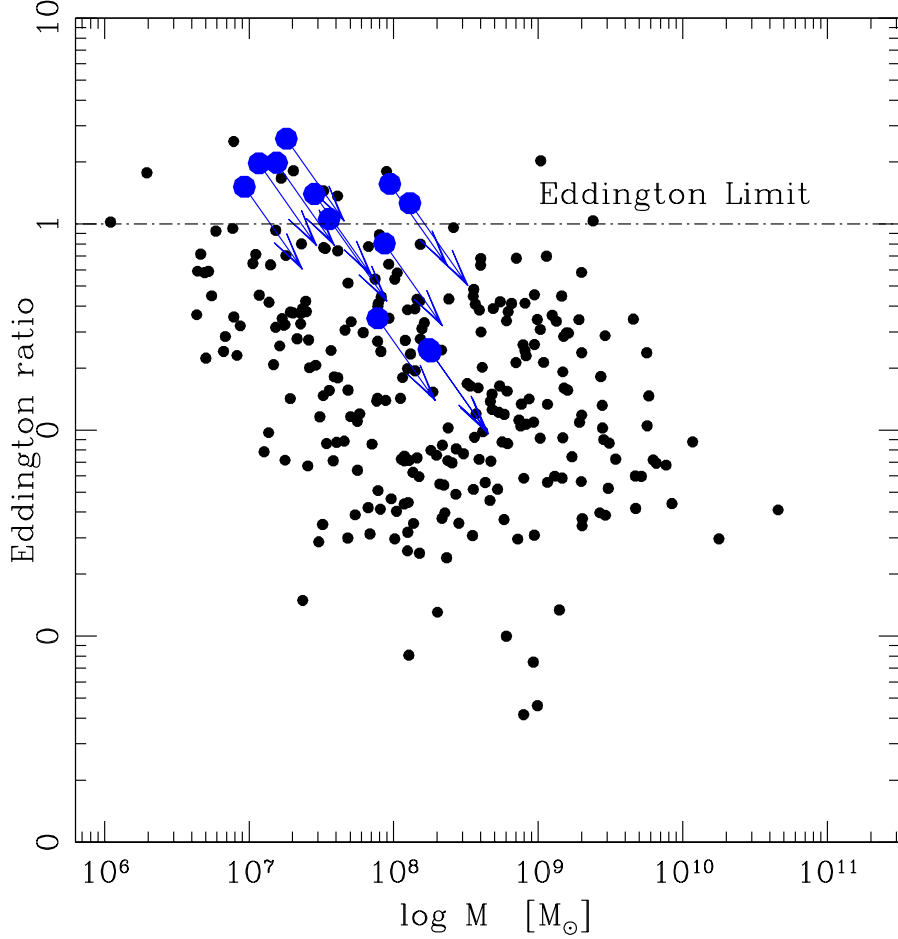


Figure 3: Effects of orientation on the low- $z$  sample of Marziani et al. (2003b). Blue outliers (large blue spots) are indicated along with other sources in our sample (filled circles) in the plane  $L/L_{\text{Edd}}$  vs.  $M_{\text{BH}}$ . The largest circle indicates the position of PKS 0736+01, a radio-loud blue outlier. Arrows indicate displacements of blue outliers if we apply an orientation correction to their masses.

Measures of both radio-quiet and radio-loud quasars likely suffer from inclination effects with the latter offering a rather straightforward way of estimating its amplitude. One can compare average FWHM  $\text{H}\beta$  values for core-dominated and lobe-dominated sources. If the radio jet is oriented perpendicular to a flattened distribution of line emitting clouds then core- and lobe-dominated represent sources where the disk is viewed near and far from

face-on respectively. Lobe-dominated sources are found to be broader by a factor 2 (Miley and Miller, 1979; Sulentic et al., 2003; Zamfir et al., 2008). The assumption of an isotropic velocity component combined with a rotational one roughly envelops the distribution of radio-loud sources in the plane  $R$  vs FWHM  $H\beta$  parameter plane (Wills and Browne, 1986). In a small subsample of radio-loud sources with detected superluminal motion the apparent speed can be used to retrieve the angle  $\theta$  between the line-of-sight and the relativistically moving plasma, once an estimate of the Lorentz factor  $\gamma$  is obtained in the framework of the synchrotron self-Compton model of X-ray and radio emission (Rokaki et al., 2003; Sulentic et al., 2003). A diagram of  $\theta$  vs. FWHM confirms a factor  $\gtrsim 2$  broadening for the sources observed at larger inclination. An effect of similar amplitude is expected for radio-quiet sources, although attempts have yet to yield a convincing orientation indicator (see however the recent work of Boroson 2011). Considering that  $\theta$  may be in the range *few degrees*  $\lesssim \theta \lesssim 45^\circ$ , and distributed randomly, we can have an average  $\langle \theta \rangle \approx 30^\circ$ ; this means that, ignoring orientation effects leads to an underestimate of the mass for almost all sources, up to a factor  $\sim 10$  if the source is observed almost pole-on and if the BLR is strongly flattened. The effect is less (a factor  $\approx 5$ ) in the case of Pop. B sources where a vertical component of motion (possibly due to turbulence) is more strongly affecting the line width (e.g., Gaskell, 2009b). Even if pole-on sources are rarest in a randomly-oriented sample, errors of this amplitude may dramatically increase the scatter in large samples and influence inferences on Eddington ratio (Jarvis and McLure, 2006). Fig. 3 shows the rare population of “blue outliers” i.e., Pop. A sources showing a large  $[OIII]\lambda\lambda 4959, 5007$  blueshift (Zamanov et al., 2002) and believed to be oriented almost pole-on (Boroson, 2011). If broad  $H\beta$  is emitted in a highly flattened configuration then they will appear systematically undermassive and hence super-Eddington. An orientation correction of 0.4 (in logarithm) to estimated masses of the blue outliers moves them in the sub-Eddington regime of  $L/L_{\text{Edd}}$  vs  $M_{\text{BH}}$  diagram.

#### 4. BLR radius from Reverberation Mapping

The last 25 years (the first recorded attempt is due to Gaskell, 1988) saw the rise of reverberation mapping based estimates of  $M_{\text{BH}}$  and many reviews can be found on this technique (Peterson, 1993; Peterson and Horne, 2006; Peterson, 2008). The cross-correlation function between continuum and emission-line light curves yields a time lag measure  $t$  (Gaskell and Sparke,

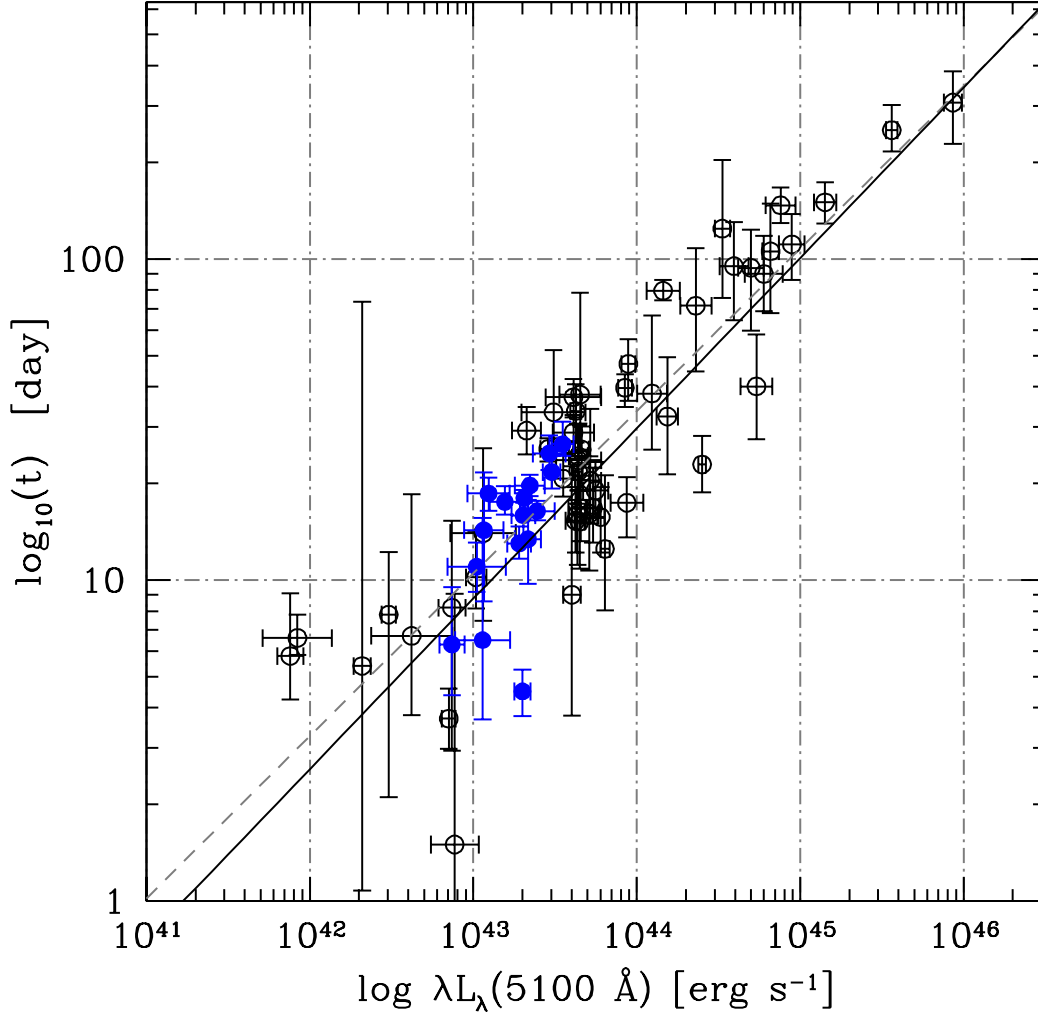


Figure 4: Correlation between time delay in units of day and luminosity at 5100 Å in units of  $\text{erg s}^{-1}$ . Original data from Bentz et al. (2009); separate determinations for the same object are shown as independent points. The filled (blue) circles refer to NGC 5548; the dashed line is an unweighted least square fit. The filled line is a least-square fit weighted over the uncertainty in  $\log t$ .

1986). The time lag due to the light travel time across the broad line emitting region yields an estimate of  $r_{\text{BLR}} = ct$  (Lyutyi and Cherepashchuk, 1972;

Cherepashchuk and Lyutyi, 1973). One can then derive the black hole mass using FWHM  $H\beta_{\text{BC}}$  under the assumption of virialized motions, using Eq. 3. Here we will focus on the accuracy of such  $M_{\text{BH}}$  estimations. The measure of  $r_{\text{BLR}}$  is based upon several assumptions (Gaskell and Sparke, 1986; Krolik, 2001; Marziani et al., 2006).

1. The continuum emitting region is much smaller than the line emitting region. This assumption might not be satisfied since the width of the continuum autocorrelation function is usually not much less than the measured delay. If the continuum is emitted by the accretion disk, the region emitting the optical continuum might reach the inner BLR (see Table 1 of Gaskell, 2008). However, the autocorrelation function of the ionizing continuum (usually not observed) might well be narrower than the one considered in most reverberation studies (see e.g., Gaskell, 2008, for a review). For  $H\beta$ , the continuum might be monitored with broad band photometry, or one may measure the specific continuum flux at a suitable wavelength;
2. The observed continuum and the  $\text{H}\text{I}$  ionizing continuum are directly related. The latter assumption appears to be valid, since the monochromatic luminosity at selected UV wavelengths has been shown to strongly correlate with the BLR radius by the international AGN Watch campaigns (Clavel et al. 1991; Peterson et al. 1991; Edelson et al. 1996; see also McLure and Jarvis 2002; Vestergaard 2002 and Gaskell 2008 for an analysis of NGC 7469, the only object for which a significant time delay between the optical and UV continuum was found).
3. The light travel time across the BLR is shorter than the dynamical response time  $t_{\text{dyn}}$  (so that BLR structure does not change over the light travel time). This has been verified by the monitoring campaigns.
4. No measurable dynamical effects due to radiation pressure are present. This is probably the case for relatively short time lapses ( $\leq 1$  yr in nearby Seyfert 1 galaxies) i.e., a timescale shorter than  $t_{\text{dyn}} \sim r_{\text{BLR}}/\Delta v_r \approx 4$  yr in the case of NGC 5548, by far the most extensively monitored object.
5. There is a well-defined radius that characterizes the BLR. A source of intrinsic uncertainty involves the likelihood that the BLR is not a thin shell of gas at the estimated  $r_{\text{BLR}}$  but a rather thick and stratified structure. This means that the power spectrum of spatial frequencies in the cross correlation function of continuum and line data can be

complex.

6. The line response is linear. The responsivity of the Balmer lines are generally anticorrelated with the incident photon flux (Pronik and Chuvpov, 1972). Thus, the responsivity varies with distance in the BLR for fixed continuum luminosity and it can change with time as the continuum varies (Korista and Goad, 2004). This effect might help isolate a particular region that is truly virial.
7. Line emission is roughly isotropic. This assumption is unlikely to hold for Balmer lines. In this case the angular pattern of emissivity should favor the irradiated face of the line emitting cloud (Ferland et al., 1992).

More technical problems involve unevenly sampled data, errors in flux calibration, normalization of spectra (different setup, aperture effects), and dilution by stellar continuum (Peterson, 1993; Horne et al., 2004; Bentz et al., 2006, 2009). This last problem has been found to seriously affect estimates of the index in the  $r_{\text{BLR}}-L$  relation. According to Krolik (2001), effects of a broad radial emissivity distribution (item 3), an unknown degree of anisotropy (item 7), and poor sampling in line and continuum monitoring can cause additional *systematic errors* in  $M_{\text{BH}}$  determination as large as a factor of 3 or more in either direction.

With reference to item 4, things appear to be different on a timescale longer than a couple of years. Looking in more detail at the behavior of NGC 5548, and separating the 13 years of data points of continuum and  $\text{H}\beta$  flux on a year-by-year basis reveals a distinct correlation between time delay and continuum flux (Peterson et al., 2002). The BLR appears to breath in response to continuum changes involving a significant change in  $r_{\text{BLR}}$  by a factor 3 if we exclude some outlying data points. Even if the line width decreases with increasing  $r_{\text{BLR}}$  (as expected for virial motions), an application of Eq. 3 yields a somewhat different mass at each epoch when the continuum luminosity is different – in principle an absurd result. Using the data for  $\text{H}\beta$  of NGC 5548 (Peterson et al., 2004), we find that  $M_{\text{BH}}$  changes by a factor 4 if the year-by-year data are separately used. If they are averaged together,  $\overline{M_{\text{BH}}} \approx (1.3 \pm 0.3) \cdot 10^7 M_{\odot}$ , where the uncertainty is at  $1\sigma$  confidence level and could be taken as indicative of the *maximum statistical accuracy* achievable on the virial product  $r_{\text{BLR}}\sigma^2$  using the reverberation method.

We remark that this degree of accuracy is not possible for the wide majority of the sources with  $r_{\text{BLR}}$  determination from reverberation data. A major limitation of the reverberation technique involves the need for many

spectra of an individual source and spectra spaced across a large enough time interval to capture well-defined continuum fluctuations and subsequent line responses. This requirement led to a worldwide campaigns that resulted in reverberation measures for  $H\beta$  of more than 60 low  $z$  sources (Bentz et al., 2009, 2010; Denney et al., 2010). Only a few sources were observed in campaigns that allowed two or more independent determinations of  $M_{\text{BH}}$ . Differences in derived  $M_{\text{BH}}$  can be as large, a factor 3 for Mark 817 and a factor 2 for Mark 110 (Peterson et al., 2004).

There is a tight correlation between X-ray variability amplitude and  $M_{\text{BH}}$  estimates for sources with  $H\beta$  reverberation data. The intrinsic dispersion in a best-fit linear relation is 0.2 dex (Zhou et al., 2010). The method based on X-ray variability relies on the assumption that the X-ray variability timescale correlates with source size (e.g., Hayashida et al., 1998; Nikolajuk et al., 2004). The X-ray method has the advantage that it does not rely on the virial assumption. The agreement is very good and the rms scatter quoted above is probably representative of a *typical statistical accuracy* of  $M_{\text{BH}}$  values derived from the reverberation method.

A few reverberation measures of  $\text{CIV}\lambda 1549$  also exist using IUE (e.g., Gaskell and Sparke 1986; Koratkar and Gaskell 1991; Turler and Courvoisier 1998 and the early International AGN Watch campaigns e.g., Clavel et al. 1991; Korista et al. 1995) and HST (Peterson et al., 2004). However, the  $\text{CIV}\lambda 1549$  line profile is probably composed of one or more components whose broadening is either non-virial (Sulentic et al. 2007; see also § 7.2) or affected by scattering (e.g., Gaskell and Goosmann, 2008). The interpretation of the  $\text{CIV}\lambda 1549$  reverberation data is therefore expected to be even more complex than the one of  $H\beta$ . Unambiguous results may be possible only if velocity resolved reverberation mapping is carried out.

## 5. A more widely applicable technique: $M_{\text{BH}}$ scaling with luminosity

### 5.1. The $r_{\text{BLR}}$ - $L$ correlation

Clearly we need a technique that can provide reasonable estimates for the BLR radius in many hundreds or even thousands of quasars. Virial estimation appears to be the obvious and only way to accomplish this goal but we require a faster way to obtain estimates of  $r_{\text{BLR}}$  for large numbers of sources. Reverberation radii are rare and extremely rare for high luminosity ( $\log L_{5100\text{\AA}} > 45$ ) quasars which are the sources for which we are currently

able to carry out only single-epoch FWHM  $H\beta$  measurements beyond  $z \sim 0.7$ . We proceed to correlate all reverberation values with measures of source luminosity. The resultant relation (Kaspi et al., 2000, 2005; Bentz et al., 2009) provides a secondary estimate of  $r_{\text{BLR}}$ . We assume that the BLR scales with luminosity beyond  $\log L \approx 45$  so that the relation defined for low luminosity quasars can be directly employed for quasars up to 2 dex higher luminosity. It is now standard practice to estimate the BLR radius by assuming

$$r_{\text{BLR}} \propto (\lambda L_{\lambda})^a. \quad (5)$$

The exponent in the correlation between source luminosity  $L$  and  $r_{\text{BLR}}$  is  $0.5 \lesssim \alpha \lesssim 0.7$ , where  $a \approx 0.7$  was obtained by Dibai (1977). The exponent has usually been assumed to be  $a=0.5 - 0.7$ , with  $a \approx 0.52$  now considered the most reliable value (Bentz et al., 2009). Any deviation from this value has quantitative effects that are rather modest. If a restriction is made to the most likely range,  $0.5 \lesssim \alpha \lesssim 0.6$ , the effect on  $M_{\text{BH}}$  estimates is  $\approx 0.3$  dex over three orders of magnitude in luminosity.

If we employ  $H\beta$ ,  $L_{\lambda}$  is the specific luminosity at  $5100 \text{ \AA}$  in units of  $\text{erg s}^{-1} \text{ \AA}^{-1}$ , the most homogenous sample available to-date yields the relation shown in Fig. 4.

It is important to stress that the relation is mainly based on low  $z$  ( $\lesssim 0.4$ ) quasars and that the high (and low) luminosity ends of the correlation are poorly sampled. Considering only sources in the range  $43 \lesssim \log L/L_{\odot} \lesssim 45$  (i.e. where sources in Bentz et al. 2009 show uniform sampling), we still have two orders of magnitude to go in order to reach the most luminous quasars. Efforts are now underway for long term monitoring of high-luminosity quasars, although they have yet to produce significant results (Botti et al., 2010; Kaspi et al., 2007; Trevese et al., 2007). Similarly, there is a program attempting to cover the lower and middle luminosity range of the correlation, the Lick AGN Monitoring Project (LAMP) (Greene et al., 2010a; Bentz et al., 2010; Denney et al., 2010). As it is evident from Fig. 4 where yearly derivations of  $r_{\text{BLR}}$  for NGC 5548 are shown in blue, there will be some irreducible intrinsic scatter. Using the  $L$ - $r_{\text{BLR}}$  relation yields a loss of accuracy for  $M_{\text{BH}}$  estimation; from Fig. 4 one infers that the scatter is at least a factor 2 at a  $2\sigma$  confidence level at  $\log L \approx 43.5$ , although a factor 6 seems possible at lower luminosity where data points may also begin to deviate from linearity.

Fig. 5 shows FWHM  $H\beta$  as a function of luminosity for several samples,



including the high-luminosity sample described in Marziani et al. (2009). The minimum FWHM  $H\beta$  apparently increases with luminosity. The plotted lines refer to an  $r_{\text{BLR}} - L$  relation with indices  $a = 0.52$  and  $a = 0.67$ , assume virial motion and sources at each  $L$  radiating at Eddington limit (i.e., the limiting curve are not an effect of any flux-limit condition). In principle, the trend observed can be used to constrain the exponent of the  $r_{\text{BLR}} - L$  correlation if large samples of high- $L$  quasars are used. The data presented in Marziani et al. (2009) for intermediate  $z$  quasars apparently favor a value larger than  $a = 0.52$ , although the lowest-FWHM points could be due, for example, to orientation effects (§3.3).

### 5.2. $M_{\text{BH}} - L$ relations

The correlation between  $r_{\text{BLR}}$  and luminosity has been redefined for the UV continua luminosity appropriate for using the width of UV lines as a virial broadening estimator. This simply means to compute a best fit between continuum at 3000 Å for  $\text{MgII}\lambda 2800$  (or at 1350 Å for  $\text{CIV}\lambda 1549$ ) and the  $H\beta$ -based  $r_{\text{BLR}}$  (e.g., McLure and Jarvis, 2002; McLure and Dunlop, 2004; Vestergaard and Peterson, 2006; Shen et al., 2008; Rafiee and Hall, 2011).

Vestergaard and Peterson (2006) derived mass scaling relations from the empirical  $r_{\text{BLR}} - L$  relation that have been used to compute  $M_{\text{BH}}$  for large samples of quasars with single-epoch  $H\beta$  or  $\text{CIV}\lambda 1549$  observations. Vestergaard and Peterson (2006) then applied the scaling relations to the objects whose  $r_{\text{BLR}}$  is available from reverberation mapping. They found that the statistical accuracy of  $M_{\text{BH}}$  mass estimates is low,  $\approx \pm 0.66$  and  $\approx \pm 0.56$  at a  $\pm 2\sigma$  confidence level for  $H\beta$  and  $\text{CIV}\lambda 1549$  respectively. Improvements could come from a more refined consideration of the virial broadening estimator for single epoch observations (§6).

## 6. Virial broadening and distinguishing quasar populations

Single epoch measures of FWHM are not necessarily the best estimators of the BLR velocity dispersion. The highest precision measure of the virial product involves emission-line width obtained using the cross-correlation function centroid (as opposed to the cross-correlation function peak) for the time delay and line velocity dispersion  $\sigma$  (as opposed to FWHM) for the line width. Obviously one wants to measure the line width in the variable part of the profile. This is the part most likely to be optically-thick to the Lyman continuum and therefore responding to continuum changes. Peterson et al. (2004)

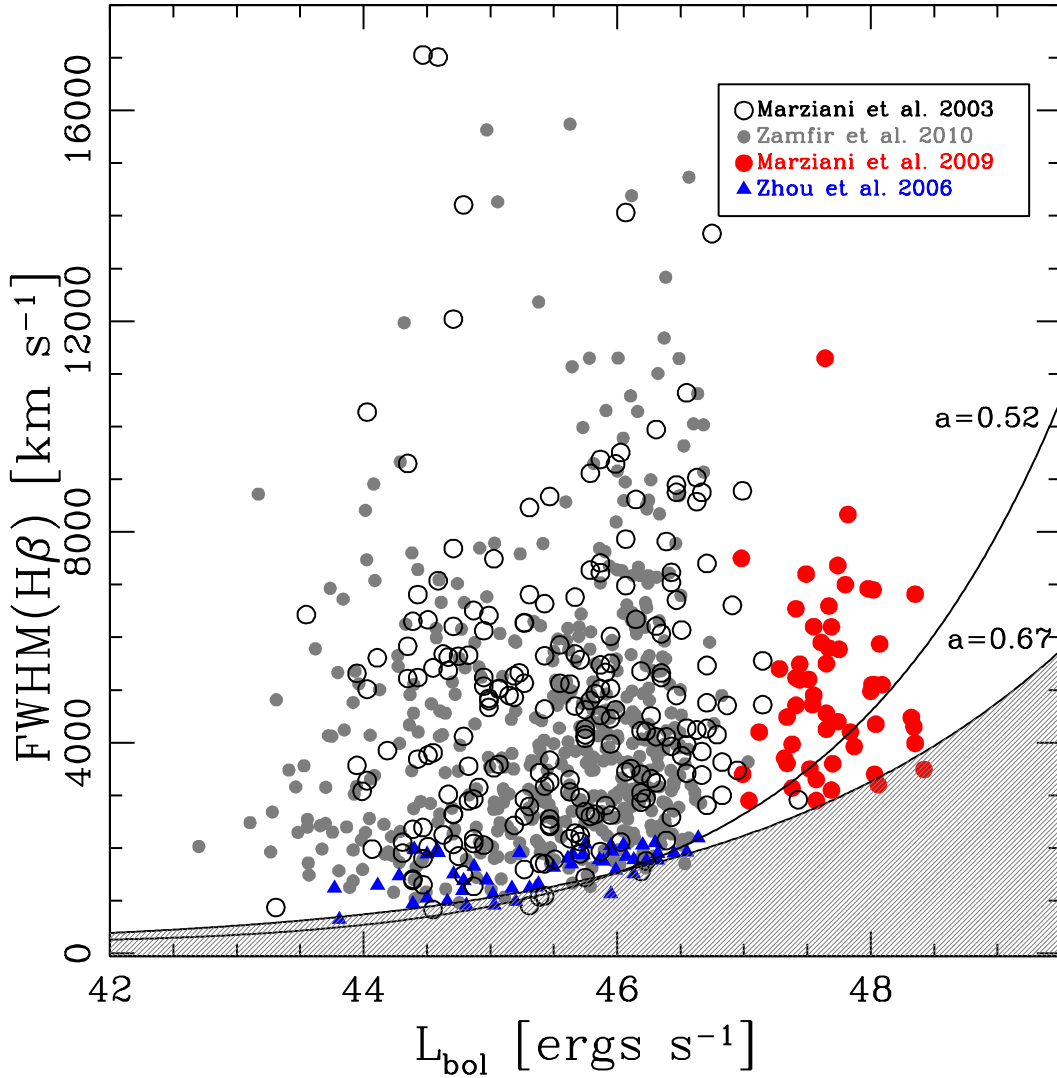


Figure 5: FWHM as a function of bolometric luminosity reported for two low- $z$  samples and the high-luminosity, intermediate  $z$  sample of Marziani et al. (2009). The last sample is based on high  $s/n$  observations of  $\text{H}\beta$  with the IR spectrometer ISAAC at VLT (Moorwood et al., 1998). The shaded area emphasizes an apparent avoidance zone where no source is expected if quasars do not radiate super-Eddington, and the exponent of the  $r_{\text{BLR}}-L$  scale relation is  $a \approx 0.67$ . Given that the relevant trend is for the *minimum* FWHM as a function of  $L_{\text{bol}}$ , we show the narrowest sources of a large SDSS sample of NLSy1s (Zhou et al., 2006). These sources also follow the expected minimum FWHM dependence on  $L_{\text{bol}}$ . Adapted from Marziani et al. (2009).

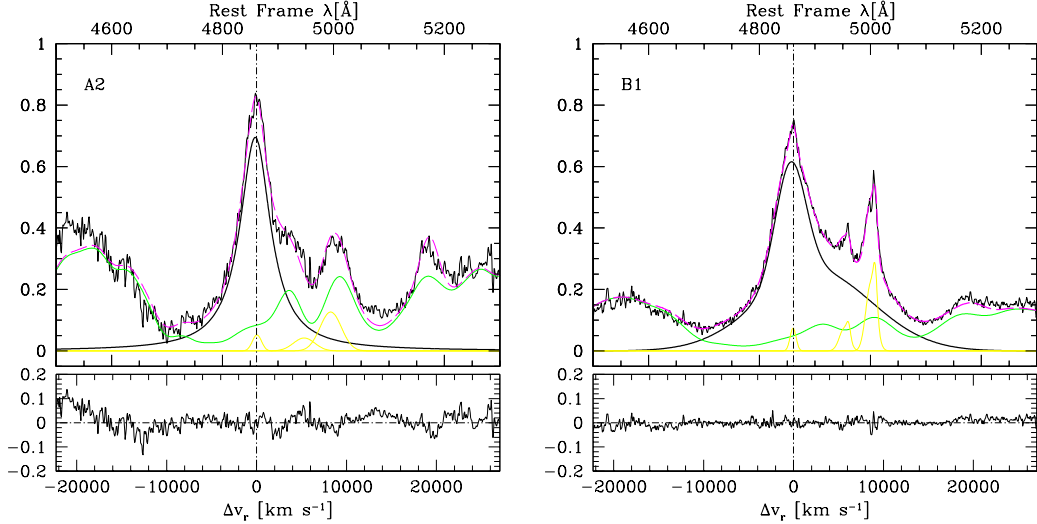


Figure 6:  $H\beta$  profiles in spectral types A2 and B1 that are typical of Pop. A and B respectively. The displayed median spectra have been computed from a large sample of SDSS high  $s/n$ , low- $z$  quasars (Sulentic et al., in preparation).

found that that the rms  $\sigma$  minimizes the random component of errors in reverberation-based  $M_{\text{BH}}$  measurements (with an absolute minimum around 30% for NGC 5548, as discussed in §4), so that rms  $\sigma$  is probably the best choice.

Which measurement is better in general for single epoch spectra, FWHM or  $\sigma$ ? FWHM is very straightforward; however it is sensitive to substructures in the profile (e.g., double peaked profiles), and presence of inflections that can yield unstable values depending on continuum placement. On the converse,  $\sigma$  has the significant disadvantage of diverging in profiles with prominent line wings (and to be  $\rightarrow \infty$  for Lorentzian profiles). Especially in the case of low  $s/n$ ,  $\sigma$  values are affected by large errors.

One must at least consider that the ratio  $\text{FWHM}/\sigma$  changes with line width (Collin et al., 2006) and avoid mixing all sources together in large samples (e.g., Nagao et al., 2006). The change occurs when radiative and gravitational forces appear to balance (Eq. 4):  $L/L_{\text{Edd}} \approx 0.15 \pm 0.05$  (Marziani et al., 2003b) for  $N_c = 10^{23} \text{ cm}^{-2}$ , probably an appropriate average value of column density.

### 6.1. $H\beta$ in Population A Sources

Pop. A profiles ( $\text{FWHM } H\beta < 4000 \text{ km s}^{-1}$ ) are well fit by a single component Lorentz function (Gaussians yield larger residuals; Véron-Cetty et al., 2001; Sulentic et al., 2002; Marziani et al., 2003b) and tend to show lower amplitude variations and less change in profile shape when continuum varies (compared to Pop. B(roader) sources; Klimek et al. 2004; Ai et al. 2010). One can describe them as Narrow Line Seyfert 1-like sources. The biggest challenge for extracting an accurate FWHM measures from Pop. A profiles involves careful subtraction of the usually strong FeII emission that afflicts and broadens the red side of the profile. Line profile shifts or asymmetries are usually small.

### 6.2. $H\beta$ in Population B Sources

The typical Pop. B  $H\beta$  line ( $\text{FWHM } H\beta > 4000 \text{ km s}^{-1}$ ) is more complex and requires two Gaussian component models to adequately describe the profile (Fig. 6). The narrower, broad component is likely the most reliable virial estimator while the VBC component showing a redshift of 1000 - 2000  $\text{km s}^{-1}$  and  $\text{FWHM } 10000 \text{ km s}^{-1}$  is unlikely to be virial. The narrower component then is viewed as the classical BLR component which is the only one seen in Pop. A sources. As for Pop. A, usually shifts are small although one must consider that a fraction of Pop. B sources show shifts that are significant relative to the line width; Zamfir et al. 2010). It apparently reverberates more strongly than the VBC (e.g., Sulentic et al., 2000b; Korista and Goad, 2004). The VBC can affect both estimates of  $r_{\text{BLR}}$  and virial velocity for almost half of quasars. It must be taken into account during reverberation studies or it will slow down and/or blur the CCF results; it must be considered in measures of  $\text{FWHM } H\beta$  or the virial velocity can be seriously overestimated (factors of 2 or 3). The relative strengths of the two  $H\beta$  components appears to depend on source luminosity (Marziani et al., 2009; Meadows et al., 2011) with the VBC becoming more dominant in high luminosity quasars. This is obviously important for studies of  $r_{\text{BLR}}$  and  $M_{\text{BH}}$  as a function of  $L$  and  $z$ . As spectral s/n decreases the two components are unlikely to be recognizable with the result that  $\text{FWHM } H\beta$  will be systematically overestimated.

## 7. Mass estimates for large samples

We must examine all strong broad lines as potential virial estimators. In the following, this review focuses on attempts to estimate  $M_{\text{BH}}$  for large numbers of quasars over as wide as possible range of redshift and source luminosity. Opinions will vary about how far we have succeeded in this quest.

Whether Pop. A or B, the number of sources with reliable FWHM  $\text{H}\beta$  measures becomes increasingly small above  $z \approx 0.7$ . One is left with three options if one wishes to study sources at higher redshift: (1) follow  $\text{H}\beta$  into the infrared, or (2) adopt other broad lines (e.g.  $\text{MgII}\lambda 2800$  or  $\text{CIV}\lambda 1549$ ) as surrogate virial estimators. If one wishes to study lower luminosity sources at low redshift then option (3) involves using databases like SDSS where contextual binning of many source spectra can yield high s/n profiles (see e.g. Zamfir et al., 2010; Meadows et al., 2011). The availability of infrared spectrographs at 4m+ class telescopes makes option (1) possible for tens or even hundreds of sources. By “possible” we mean that it becomes possible to obtain spectra with s/n ( $\sim 20$  in continuum near  $\text{H}\beta$ ) comparable to lower redshift optical measures for the brightest individual SDSS (or other) spectra. Using ESO VLT and IR spectrometers like ISAAC one can presently obtain such spectra for sources at the bright tip of the quasar luminosity function up to  $z \lesssim 3.8$  with exposure times of  $\sim 40$  minutes. The availability of IR windows determines the source redshift distribution using  $\text{H}\beta$  but reasonable coverage over the range  $z = 1 - 3.8$  is possible. The advantage of this approach is uniformity, same reduction procedure and same virial estimator.

The SDSS database is a seductive source of data for more than 100000 quasars offering the possibility to derive instant  $M_{\text{BH}}$  estimates. Beyond the brightest  $\approx 500$  sources this is an illusion as the decline in s/n makes reliable FWHM estimates increasingly difficult. If all quasar spectra were basically the same then one could proceed by fitting profile models, determined for the brightest sources, to large numbers of noisy spectra. We now know that spectra of quasars are less similar than are stellar spectra along the main sequence of the H-R Diagram. Dissimilarities include:

1. internal broad (and narrow) line shifts,
2. the line profiles at a fixed redshift or source luminosity show large differences as detailed earlier,
3. FeII contamination varies widely and directly affects the FWHM measure.

Quite aside from arguments about the validity of any specific line as a virial estimator, the SDSS database of spectra (all but 100s) can be used but only if the data are binned into some well defined context (for example the spectral type defined by Sulentic et al. 2002), or some innovative approach is applied (e.g., Rafiee and Hall, 2011).

### 7.1. *Mass estimation using $\text{MgII}\lambda 2800$*

McLure and Dunlop (2004) computed virial black hole mass estimates for a sample of more than 10000 quasars in the redshift interval  $0.1 < z < 2.1$  drawn from the SDSS Quasar Catalogue of Schneider et al. (2003). The  $\text{H}\beta$  line was used up to  $z \approx 0.7$ , and  $\text{MgII}\lambda 2800$  beyond. The change in virial estimator did not introduce any obvious discontinuity. Also no evidence of large masses exceeding the  $M_{\text{BH}}$  of locally detected dormant black holes were found. This behavior is not surprising since  $\text{H}\beta$  and  $\text{MgII}\lambda 2800$  are both LILs thought to be produced mostly in the same emitting region. There is evidence that the  $\text{MgII}\lambda 2800$  FWHM distribution might be narrower than the one of  $\text{H}\beta$  (Labita et al., 2009), and that individual  $\text{MgII}\lambda 2800$  FWHM values are systematically narrower than  $\text{H}\beta$  (Wang et al., 2009). If so (and if the presence of narrow absorptions on the blue side of  $\text{MgII}\lambda 2800$  are not creating a spurious effect),  $\text{MgII}\lambda 2800$  might be more appropriate because its single epoch profile may be a better approximation of the reverberating part of  $\text{H}\beta$  isolated on the rms spectrum, as also suggested for  $\text{FeII}$  (Sulentic et al., 2006).

### 7.2. *(Dangerous) mass estimation using $\text{CIV}\lambda 1549$*

Much more controversial has been the use of  $\text{CIV}\lambda 1549$  as a virial broadening estimator (Baskin and Laor, 2005; Netzer et al., 2007).

The most serious effect is related to the strong blueshift with respect to the rest frame frequently observed in  $\text{CIV}\lambda 1549$  (Gaskell, 1982; Richards et al., 2011). This suggests that either the high-ionization line emitting gas is out-flowing in a wind (Gaskell, 1982; Marziani et al., 1996) in at least a significant fraction of quasars and hence not in virial equilibrium, or that there is some other broadening mechanism, such as electron scattering or Rayleigh scattering (Gaskell and Goosmann, 2008). In either case  $\text{CIV}\lambda 1549$  is not a reliable mass indicator. This fraction may even increase with redshift and luminosity, judging from the observed  $\text{CIV}\lambda 1549$  profile in a high  $z$  quasar sample Barthel et al. (1990). The effect is very pronounced if we consider a prototypical source believed to accrete close to the Eddington limit, I Zw 1

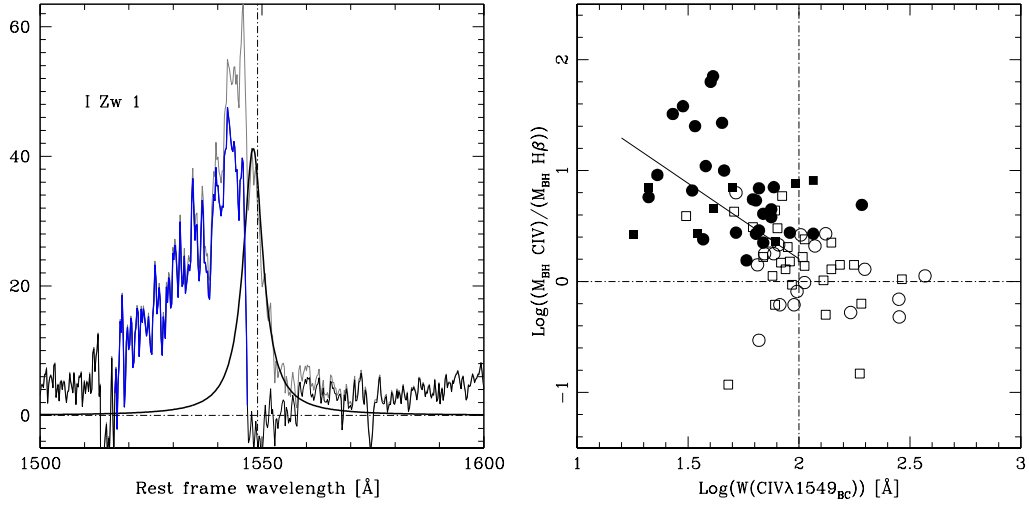


Figure 7: Left:  $\text{CIV}\lambda 1549$  and  $\text{H}\beta$  profile of the prototype Pop. A source I Zw 1. The grey line represents the original profile, the black one the scaled  $\text{H}\beta$  profile and the blue solid line the residual after subtraction of the scaled  $\text{H}\beta$  profile. The ratio between  $M_{\text{BH}}$  computed using  $\text{FWHM CIV}\lambda 1549$  and  $\text{FWHM H}\beta$  as virial broadening estimators as a function of  $W(\text{CIV}\lambda 1549)$ . Filled circles: Pop. A radio-quiet sources; filled squares: Pop. A radio-quiet; open circles: Pop. B radio-quiet; open squares: Pop. B radio-loud. Adapted from Sulentic et al. (2007).

(Fig. 7). The C IV  $\lambda 1549$  profile can be modeled as an the unshifted almost symmetric H $\beta$  profile plus a prominent blueshifted component. The broadening, in this case, is dominated by a shifted non-virial component. Since  $M_{\text{BH}} \propto (\delta v)^2$ , the effect can reach a factor 10 on  $M_{\text{BH}}$ , as shown in the right panel of Fig. 7. For Pop. B sources, there is no obvious systematic effect, although the  $M_{\text{BH}}$  derived from C IV  $\lambda 1549$  is sometime much lower than the one derived from H $\beta$ , probably because of significant C IV  $\lambda 1549$  narrow emission (C IV  $\lambda 1549_{\text{NC}}$ ).

The very existence of C IV  $\lambda 1549_{\text{NC}}$  has been a contentious issue. Radio-loud sources often show prominent C IV  $\lambda 1549$  cores of width  $\sim 2000 \text{ km s}^{-1}$ , but such emission has been ascribed to C IV  $\lambda 1549_{\text{BC}}$  (Wills et al., 1993) and to an intermediate line region (Brotherton et al., 1994). We have interpreted this feature as part of the NLR, and recent detection of narrow C IV  $\lambda 1549$  in high  $z$  type-2 sources supports this interpretation (e. g., Mainieri et al., 2005; Severgnini et al., 2006). Provided that a smooth density gradient exist (i.e., that there is a significant amount of gas at  $n_e \sim 10^6 \text{ cm}^{-3}$ , we expect C IV  $\lambda 1549$  emission to be strong (C IV  $\lambda 1549$  emissivity is  $\propto n_e^2$  while [O III]  $\lambda\lambda 4959, 5007$  should become collisionally quenched). If velocity dispersion increases with decreasing distance from the central continuum source, as expected if there is at least rough virial equilibrium, then it is somewhat natural to expect  $\text{FWHM}(\text{C IV } \lambda 1549_{\text{NC}}) > \text{FWHM}([\text{O III}] \lambda\lambda 4959, 5007)$  (De Robertis and Osterbrock, 1986; Appenzeller and Oestreicher, 1988; Sulentic and Marziani, 1999).

A comparison of FWHM H $\beta_{\text{BC}}$  and C IV  $\lambda 1549$  line shift measures with those of other workers (Warner et al., 2004; Baskin and Laor, 2005) shows that significant and systematic differences exist between the measures. FWHM C IV  $\lambda 1549_{\text{BC}}$  measures begin to deviate towards smaller values at FWHM C IV  $\lambda 1549 \sim 4000 \text{ km s}^{-1}$  where we believe that the NLR becomes important (Pop. B; Bachev et al. 2004). However, considering the strong Baldwin effect that is observed in [O III]  $\lambda 5007$  (mainly due to the increasing rarity of [O III]  $\lambda 5007$ -strong objects at high luminosity Netzer et al. 2004; Kovačević et al. 2010; Sulentic et al., in preparation), the relevance of C IV  $\lambda 1549_{\text{NC}}$  could be small in high  $z$  quasars, for which C IV  $\lambda 1549$  becomes the only line available for estimating the virial broadening from optical observations.

Concluding, the FWHM of C IV  $\lambda 1549$  is a poor virial broadening estimator subject to systematic biases. Alternatively the intermediate ionization lines (especially Si III  $\lambda 1892$  and Al III  $\lambda 1860$ ) could in principle be used even if blended. Intermediate-ionization lines like Si III  $\lambda 1892$  and Al III  $\lambda 1860$  show



negligible blueshifted, non virial emission, weak VBC and a profile roughly consistent with the broad component of  $H\beta$  (Marziani et al., 2010, and references therein).

## 8. Photoionization Methods

Historically, the first attempt to derive  $M_{\text{BH}}$  from photoionization conditions is due to Dibai (1977), as mentioned in §1. The underlying assumption was of course that all AGN were in similar physical conditions, so that the luminosity of  $H\beta$  could be related to the BLR size assuming an identical value of the line emissivity. The application of Eq. 1 needs an estimate of the filling factor. If spherical symmetry is assumed,  $f_f$  can be easily computed from the covering factor  $f_c$  that is observationally constrained (Wandel and Yahil, 1985).

The physical conditions of photoionized gas can be described by hydrogen numeric density  $n_{\text{H}}$  or electron density, hydrogen column density  $N_{\text{c}}$  metallicity, shape of the ionizing continuum, and the ionization parameter  $U$ . The latter represents the dimensionless ratio of the number of ionizing photons and the total hydrogen density, ionized and neutral. If we know *the product of*  $n_{\text{H}}$  (or electron density  $n_{\text{e}}$ ) and  $U$ , we can estimate  $r_{\text{BLR}}$  from Eq. 2.  $U$  can be written in terms of  $r_{\text{BLR}}$  yielding an estimate of the BLR independent of direct reverberation estimates:

$$r_{\text{BLR}} = \left( \frac{\int_{\nu_0}^{+\infty} \frac{L_{\nu}}{h\nu} d\nu}{4\pi U n_{\text{H}} c} \right)^{\frac{1}{2}} \propto \frac{1}{(U n_{\text{H}})^{\frac{1}{2}}} Q(H)^{\frac{1}{2}} \quad (6)$$

The dependence of  $U$  on  $r_{\text{BLR}}$  was used by Padovani and Rafanelli (1988) to compute central black hole masses assuming a plausible average value of the product  $n_{\text{e}}U$ . Padovani (1989) derived an average value  $\overline{U \cdot n_{\text{e}}} \approx 10^{9.8}$  from several sources for which  $r_{\text{BLR}}$  was available from reverberation mapping and for which the number of ionizing photons could be measured from multiwavelength observations. The average  $n_{\text{e}}U$  value was then used to compute black hole masses for a much larger sample of Seyfert 1 galaxies and low- $z$  quasars (Padovani and Rafanelli, 1988; Padovani et al., 1990). Multifrequency data were used to define the shape of the ionizing continuum for each individual source. Wandel et al. (1999) compared photoionization method results with those obtained via reverberation mapping and found a very good correlation between the two mass estimates.

Recently, the photoionization method of Dibai (1984) based on  $H\beta$  luminosity was reconsidered (Bochkarev and Gaskell, 2009). The original Dibai data yield very good agreement with  $M_{\text{BH}}$  estimates from reverberation-mapped sources.

A different photoionization method could be applicable to high redshift quasars. Emission lines originating from forbidden or semi-forbidden transitions become collisionally quenched above the critical density and, hence, weaker than lines for which collisional effects are still negligible. The  $\text{AlIII}\lambda 1860 / \text{SiIII}\lambda 1892$  ratio is well suited for exploring the density range  $10^{11} - 10^{13} \text{ cm}^{-3}$  which corresponds to the densest, low ionization emitting regions likely associated with the production of  $\text{FeII}$ . The ratios  $\text{SiII}\lambda 1814 / \text{SiIII}\lambda 1892$  and  $\text{SiIV}\lambda 1397 / \text{SiIII}\lambda 1892$  are independent of metallicity and sensitive to ionization. Conversely the ratio  $\text{CIV}\lambda 1549 / \text{SiIV}\lambda 1397$  is mainly sensitive to metallicity.

We computed a multidimensional grid of CLOUDY (Ferland et al., 1998) simulations (see also Korista et al., 1997) in order to derive  $U$  and  $n_{\text{H}}$ . Computation of constant value contours in the theoretical  $U$  vs.  $n_{\text{H}}$  plane of CLOUDY simulations shows convergence towards a low ionization plus high density range. Application of this method to the NLSy1 I Zw 1 and NLSy1-like sources at high redshift provides not only an independent estimate of  $nU$  but also of  $n_{\text{H}}$ ,  $U$ , and metallicity (Negrete et al., 2010).  $r_{\text{BLR}}$  values obtained with the photoionization method can be compared to the ones obtained with sources reverberation mapping. The two sets of values agree better than the values estimated using the  $r_{\text{BLR}} - L$  correlation – and this employing the very sample used to define the  $r_{\text{BLR}} - L$  correlation (Negrete, 2011).

The large uncertainty associated with the scaling relation that employs  $\text{CIV}\lambda 1549$  (present even if the  $\text{CIV}\lambda 1549$  virial component can be properly isolated) makes preferable a one-by-one  $M_{\text{BH}}$  determination based on physical properties of an emitting region that remains self-similar. The particular value of the photoionization method is that it can be applied over the full redshift range where quasars are observed.

## 9. Black Hole Mass and Host Galaxy Mass

The correlation of nuclear black hole mass with stellar bulge velocity dispersion in nearby galaxies (Ferrarese and Merritt, 2000; Gebhardt et al., 2000) suggests a constant  $M_{\text{BH}}/M_{\text{bulge}}$  ratio. This result has been extensively used (or should we better say abused?) to derive quasar  $M_{\text{BH}}$  from the ratio  $M_{\text{BH}}/M_{\text{bulge}}$  or from a proxy of the stellar velocity dispersion.

Ferrarese and Merritt (2000) relied on maser optical emission line measurements. Gebhardt et al. (2000) and Merritt and Ferrarese (2001) added masses obtained from the so-called stellar dynamics method (e.g. Kormendy, 1993; Magorrian et al., 1998). Broadly speaking, these  $M_{\text{BH}}$  determinations have the advantage that the line emitting region is partly resolved, so that a detailed analysis of geometry and orientation effects can be carried out. It is still debated whether stellar dynamics  $M_{\text{BH}}$  determinations might introduce a bias in the measured  $M_{\text{BH}}$  (Gültekin et al., 2009). However, it is more relevant in the the quasar context to assess whether a significant  $M_{\text{BH}}-M_{\text{bulge}}$  correlation exists at all, or whether it results from a bias due to the difficulty of detecting a black hole whose sphere of influence is much smaller than the telescope resolution (Gültekin et al., 2011). In other words, the correlation may refer only to the maximum  $M_{\text{BH}}$  for each  $M_{\text{bulge}}$ . The most likely condition is that the bias is mass-dependent, and most severe at low  $M_{\text{BH}}$  (i.e., higher mass black holes are more easily detected). The true (unbiased) aspect of the relation could be tight at large  $M_{\text{BH}}$  but with increasing dispersion toward lower masses.

An additional complication is that the relation between  $M_{\text{BH}}$  and  $\sigma_*$  appears to be different for barred and non-barred hosts (Graham et al., 2011, and references therein). Intrinsic dispersion at low  $M_{\text{BH}}$  and dependence on morphology could overshadow several conflicting claims e.g., a nonlinear relation between the  $M_{\text{BH}}$  and the bulge mass for PG quasars (Laor, 2001):  $M_{\text{BH}} \propto M_{\text{bulge}}^{1.53 \pm 0.14}$ . Another case is the claim that NLSy1s, often host in dwarfish galaxies (Krongold et al., 2001) and barred spirals (Crenshaw et al., 2003; Ohta et al., 2007) possess under-massive black holes (e.g., Mathur et al., 2001; Chao et al., 2008).

A similar difficulty might apply also to the correlation between black hole mass and bulge luminosity (Kormendy and Richstone, 1995): the dispersion of data at low- $L_{\text{bulge}}$  could make any correlation ill-defined (Gaskell and Kormendy, 2009; Gaskell, 2010a). The  $L_{\text{bulge}} - M_{\text{BH}}$  relation suffers from the additional problem that Seyfert galaxy hosts are brighter than normal galaxies for a

given value of their velocity dispersion, perhaps as a result of younger stellar populations (Nelson et al., 2004), even if the use of IR luminosity can greatly reduce the scatter (Marconi and Hunt, 2003).

Radio-quiet quasars seem to follow the established  $M_{\text{BH}}-\sigma_*$  relation up to  $z \approx 0.5$ , with a modest evolution in the redshift range  $0.5 \lesssim z \lesssim 1$  (Shields et al., 2003; Salviander et al., 2007). However, the  $M_{\text{BH}}/M_{\text{bulge}}$  ratio estimated at low  $z$  should not be mistaken for an universal constant. Studies at high redshift find  $M_{\text{BH}}$  and  $M_{\text{bulge}}$  values that indicate overmassive black holes at high  $z$  (Targett et al., 2011, and references therein). Evolution in the  $M_{\text{BH}}/M_{\text{bulge}}$  ratio casts doubts on the physical implications of the relation at low- $z$ .

## 10. Using [OIII] $\lambda$ 5007 as a proxy for stellar velocity dispersion

If the  $M_{\text{BH}}/M_{\text{bulge}}$  ratio can be derived with good accuracy, then  $M_{\text{BH}}$  could be computed using a proxy for  $\sigma_*$ . There are two major difficulties with using FWHM [OIII] $\lambda$ 5007 as a proxy for  $\sigma_*$ . While a  $M_{\text{BH}} - \text{FWHM [OIII]}\lambda 5007$  correlation exists (Nelson, 2000), the scatter is large. The derived values can be considerably higher than those calculated using FWHM  $\text{H}\beta_{\text{BC}}$  (Marziani et al., 2003b). On the one hand, the narrowest profiles of [OIII] $\lambda$ 5007 appear to be sub-virial in the gravitational potential of the host bulge, probably because the line emitting gas is constrained in non-spherical geometries (see the discussion in Gaskell 2009a and references therein). On the other hand, low- $W([\text{OIII}]\lambda 5007)$  sources can show  $\text{FWHM [OIII]}\lambda 5007 \gtrsim \text{FWHM}(\text{H}\beta)$ , seriously challenging the assumption of gravitational dominance by the bulge potential. Blueshifted [OIII] $\lambda$ 5007 profiles are observed and likely arise in outflowing gas (Zamanov et al., 2002), possibly associated with a disc wind. The distribution of [OIII] $\lambda$ 5007 velocity shifts with respect to [OII] $\lambda$ 3727 indicates that the majority of sources are significantly blue-shifted (Hu et al., 2008). The narrow line region (NLR) in blueshifted sources is not likely to be dynamically related to the host-galaxy stellar bulge. This is even more true for a minority of sources with  $\Delta v_r \lesssim -300 \text{ km s}^{-1}$  (the so-called blue-outliers of Zamanov et al. 2002) whose NLR may be very compact. This points to a limiting  $W([\text{OIII}]\lambda 5007) \approx 20 \text{ \AA}$  below which  $\text{FWHM}([\text{OIII}]\lambda 5007)$  emission probably ceases to be a useful mass estimator. Only large  $W([\text{OIII}]\lambda 5007)$  radio-quiet Pop. B sources may have very extended NLRs whose motions are dominated by the stellar bulge. Very appropriately, the width of the [SII] $\lambda\lambda$ 6716,5631 or [OII] $\lambda$ 3727 doublet has been

proposed as an alternative to  $[\text{OIII}]\lambda\lambda 4959, 5007$  width (Komossa and Xu, 2007; Salvander et al., 2007).

## 11. Masses from Double Peakers

A small fraction of AGN exhibit very broad and double peaked LILs. The  $\text{H}\alpha$  BC profile is strikingly peculiar (see Sulentic et al. 2000a; Eracleous and Halpern 2003; Strateva et al. 2003 for examples). Prototype double-peakers Arp 102B, 3C 390.3, and 3C 332 have been monitored for more than 20 years (Lewis and Eracleous, 2006; Gezari et al., 2007). A common property of double peakers involves variability of the profile shape on timescales of months to years. This slow systematic variability of the line profile shows similar timescales to dynamical changes expected in an accretion disk (Eracleous and Halpern, 2003; Newman et al., 1997). Five year monitoring of  $\text{H}\beta$  (Shapovalova et al., 2001) supports rejection of the binary BH hypothesis (Gaskell, 1983) for 3C390.3, on the basis of the masses required (Halpern and Filippenko, 1988). Hot spots, spiral waves and elliptical accretion disks have also been suggested (Storchi-Bergmann et al., 2003; Lewis and Eracleous, 2006).

If one can detect changes in the line profile induced by the hot spot, it is in principle possible to derive the period of the hot spot and hence to estimate  $r_{\text{BLR}}$  and  $M_{\text{BH}}$  in physical units. In the case of Arp 102B one obtains a mass  $\approx (2.2 \pm 0.7) \cdot 10^8 M_{\odot}$  for the black hole, and a distance of  $4.8 \cdot 10^{-3}$  pc ( $\approx 500 R_g$ ) for the hot spot (Newman et al., 1997). Derivation of  $r_{\text{BLR}}$  in physical units removes the degeneracy introduced by the Keplerian velocity field (i.e., the velocity scales as  $(M_{\text{BH}} / r)^{-0.5}$ , and disk model profiles yield a distance normalized to  $R_g$ ). Unfortunately, gravitational and transverse redshifts show the same dependence  $\propto (M_{\text{BH}} / r)^{-0.5}$  at first order. A gravitational redshift will not help us solve for  $M_{\text{BH}}$  and  $r$  in physical units; detection of a radial velocity change with time will do it. Monitoring has been pursued for sources showing single-peaked line profiles under the assumption that the disk contribution is masked by emission from a wind or hot spots (Bon et al., 2009; Jovanović et al., 2010). This approach provided a new estimate of the black hole mass for NGC 4151 (Bon et al., in preparation).

## 12. A binary black hole revival

A binary black hole model was originally proposed to explain sources showing double-peaked line profiles like Arp 102B (Gaskell, 1983). Lower

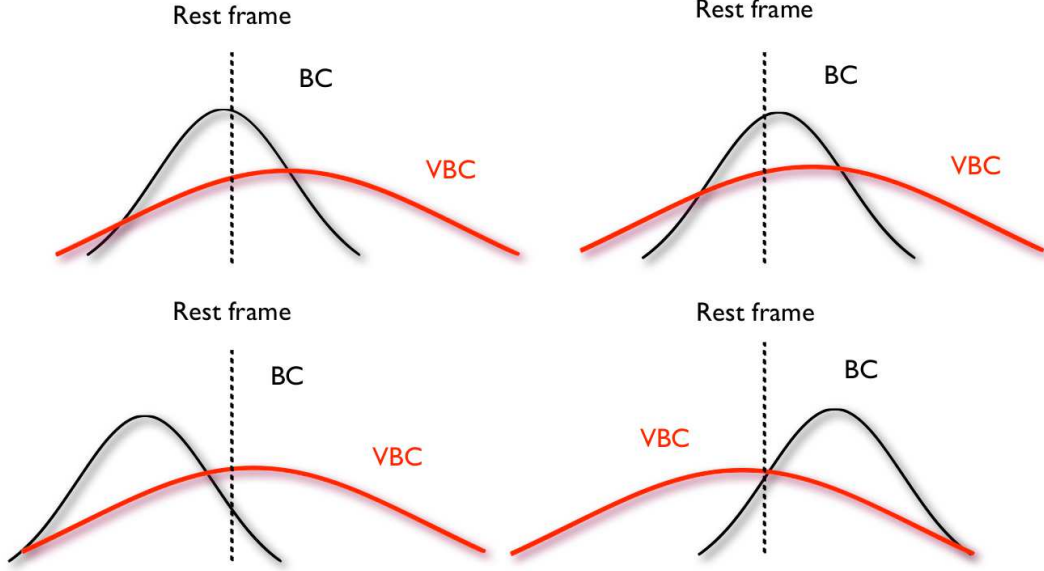


Figure 8: Sketch illustrating 2 examples of most-frequently observed  $H\beta$  profiles in Pop. B sources (upper half) and the profiles that might be signatures of binary black holes. The SDSS 153636.221+044127.0  $H\beta$  line profile (Boroson and Lauer, 2009) corresponds to the lower-left case.

limits for plausible orbital periods based on the absence of peak radial velocity changes would require supermassive binary black holes with total masses in excess of  $10^{10} M_{\odot}$  (Halpern and Filippenko, 1988; Shapovalova et al., 2001). Such large  $M_{\text{BH}}$  values are difficult to reconcile with the maximum  $M_{\text{BH}}$  values observed in the local Universe (Eracleous et al., 1997) and with the  $M_{\text{BH}} - \text{bulge mass}$  relation.

The search for supermassive binaries with sub-parsec separation has undergone a revival (Eracleous et al., 2011; Tsalmantza et al., 2011) since such binary black holes are expected in scenarios involving black hole and bulge coevolution (Begelman et al., 1980; Volonteri et al., 2009). A candidate involves the quasar SDSS J153636.221+044127.0 that shows line features possibly indicating two broad-line systems separated in radial velocity by  $3500 \text{ km s}^{-1}$ , and a system of unresolved absorption lines at intermediate radial velocity (Boroson and Lauer, 2009). A disk model with off-axis illumination has also been proposed (Gaskell, 2010b,c) for this source.

It is difficult to use a single source with almost unique<sup>1</sup> line properties to argue for a phenomenon (i.e. binary BH) expected to be common among quasars. Peculiar shifts of the kind identified by Boroson and Lauer (2009) are restricted to Pop. B sources and the most frequently observed profile showing a redward asymmetry and a peak displacement to the red is clearly unsuitable as a binary BLR signature where the NLR indicates the rest frame (Fig. 8). If we interpret the H $\beta$  BC and VBC as two different BLRs associated with the binary, and we assume that the line emitting gas forms two bound systems, then the largest shifts should be observed in the BC, the contrary of what is most frequently observed (the VBC is redshifted by  $\gtrsim 1000$  km s<sup>-1</sup>). Other systems have been selected as possible candidates, notably the ones showing opposite peak and line base displacement in radial velocity (Shen and Loeb, 2010), but altogether they account for no more than a few percent of quasars.

### 13. Toward higher and higher redshifts: the evidence for a turnover

FWHM H $\beta$  measures can provide good  $M_{\text{BH}}$  estimates out to  $z \approx 3.8$ . 8m-class telescopes yield high s/n measures for the high luminosity tail of the quasar optical luminosity function. Sampling over a wider part of the optical luminosity function (down to Seyfert 1 luminosities ( $m_V \approx -23$ ) becomes possible with the next generation of large telescopes. BH mass estimates beyond  $z \approx 3.8$  or simply larger samples beyond  $z \approx 0.7$  requires use of H $\beta$  surrogate lines. The two most used surrogates are MgII $\lambda$ 2800 and CIV $\lambda$ 1549. CIV $\lambda$ 1549 cannot be trusted but MgII $\lambda$ 2800 may be able to serve as a surrogate virial estimator for the highest redshift quasars currently known. Spectra can be obtained for  $z \approx 6$  quasars in the K band (Kurk et al., 2007).

The best  $M_{\text{BH}}$  estimates out to  $z \approx 4$  show no evidence of a turnover which would reflect the epoch when the largest black holes were still growing. Instead we see constant  $M_{\text{BH}}$  upper limit near  $\log M_{\text{BH}} \approx 9.7$  if we trust in part (which we do not) the measurements based on CIV $\lambda$ 1549 (Shen et al., 2008; Labita et al., 2009). There may be a change at higher redshift (Trakhtenbrot et al., 2011) if we consider only  $M_{\text{BH}}$  values obtained from H $\beta$  and MgII $\lambda$ 2800 measures. Fig. 9 combines a low-  $z$  sample (Zamfir et al., 2010) with samples using H $\beta$  observed with IR spectrometers (to  $z \approx 3.5$ ) and MgII $\lambda$ 2800 using optical and IR measures. We see a possible turnover in estimated  $M_{\text{BH}}$

---

<sup>1</sup>A twin of SDSS J153636.221+044127.0 is shown in Fig. 1 of Gaskell (1983).

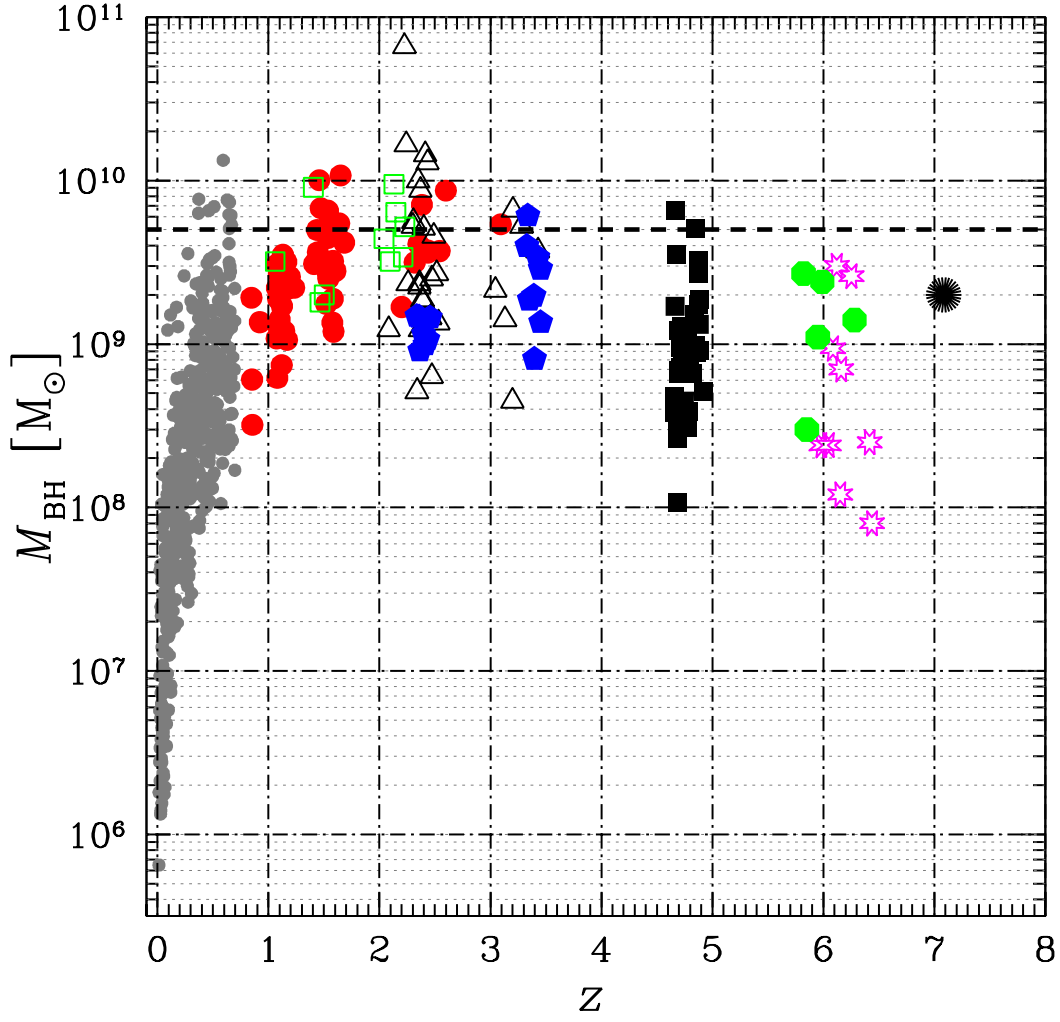


Figure 9:  $M_{\text{BH}}$  versus  $z$  for a low- $z$  sample (grey dots Zamfir et al., 2010), and several intermediate to high  $z$  samples. Red circles: Marziani et al. (2009); open squares: Dietrich et al. (2009); open triangles: Shemmer et al. (2004); filled pentagons: Netzer et al. (2007); filled squares: Trakhtenbrot et al. (2011); open starred octagons: Willott et al. (2010); filled octagons: Kurk et al. (2007); large spot at  $z \approx 7$ : the high- $z$  quasar whose discovery was announced in late June 2011 (Mortlock et al., 2011). The dashed line marks  $M_{\text{BH}} = 5 \cdot 10^9 M_{\odot}$ .



at the highest redshifts although some care is needed in interpreting these results. Most sources in the range  $1 \lesssim z \lesssim 2.5$  were selected from the brightest quasars in the Hamburg ESO survey and are the most luminous quasars known in that redshift range. Observations at very high redshift refer to much fainter quasars. We must restrict our attention to the high-end of the mass distribution when we evaluate the significance of the turnover. Counting sources with masses in the ranges  $9.25 \leq \log M_{\text{BH}} \leq 9.75$  and  $8.75 \leq \log M_{\text{BH}} \leq 9.25$ , we find that the ratio of the numbers of less-massive to more-massive sources at redshift  $\gtrsim 4$  is lower than for the samples at  $1 \lesssim z \lesssim 3.8$ . A simple application of Poisson statistics to these ratios confirms a real trend. Given the different sample selection criteria at different redshifts we believe that more data are needed before the turnover can be regarded as established.

As a final consideration we note that the computed  $M_{\text{BH}}$  may not be critical for concordance cosmology, since black holes can grow to the observed masses in a duty cycle that is significantly shorter than the age of the Universe at  $z \approx 6$  according to Trakhtenbrot et al. (2011).

## 14. Conclusion

$M_{\text{BH}}$  computation techniques for large samples of quasars are rough and the lack of accuracy in  $M_{\text{BH}}$  estimates is serious. There are several areas that could lead to significant improvement:

- a significant reduction in scatter could be achieved by more careful selection of virial broadening estimators (best are  $\text{H}\beta$  and  $\text{MgII}$ );
- a second factor is related to knowledge of the BLR structure that is still hotly debated (Gaskell, 2009b). There is evidence that Pop. A and B sources show different BLR structure and kinematics. Significantly different  $f$  values are likely associated with the two populations;
- photoionization methods should be favored over methods based on the  $r_{\text{BLR}}\text{-}L$  correlation.

Considering the large scatter introduced by uncertainties in the factors entering the virial relation it is still not surprising that  $M_{\text{BH}}$  estimates and those derived by randomly reassigning the quasar broad-line widths to different objects show such similarities in the  $M_{\text{BH}}$  vs.  $z$  plane (Croom, 2011). However this provocative result may not stand for long.

The work was presented as an invited talk at special workshop "Spectral lines and super-massive black holes" held on June 10, 2011 as a part of activity in the frame of COST action 0905 "Black holes in an violent universe" and as a part of the 8<sup>th</sup> Serbian Conference on Spectral Line Shapes in Astrophysics. We are indebted to Martin Gaskell for discussions and many insightful suggestions. We also acknowledge with gratitude the hospitality and good organization of the Conference in Divčibare (Luka, Dragana, Darko and all the others of the organizing committee).

## References

- Ai, Y.L., Yuan, W., Zhou, H.Y., Wang, T.G., Dong, X.B., Wang, J.G., Lu, H.L., 2010. Dependence of the Optical/Ultraviolet Variability on the Emission-line Properties and Eddington Ratio in Active Galactic Nuclei. *ApJL* 716, L31–L35. 1005.0901.
- Appenzeller, I., Oestreicher, R., 1988. High-ionization line profiles of Seyfert galaxies. *AJ* 95, 45–57.
- Bachev, R., Marziani, P., Sulentic, J.W., Zamanov, R., Calvani, M., Dultzin-Hacyan, D., 2004. Average Ultraviolet Quasar Spectra in the Context of Eigenvector 1: A Baldwin Effect Governed by the Eddington Ratio? *ApJ* 617, 171–183. [arXiv:astro-ph/0408334](#).
- Baldwin, J.A., Netzer, H., 1978. The emission-line regions of high-redshift QSOs. *ApJ* 226, 1–20.
- Barth, A.J., Sarzi, M., Rix, H.W., Ho, L.C., Filippenko, A.V., Sargent, W.L.W., 2001. Evidence for a Supermassive Black Hole in the S0 Galaxy NGC 3245. *ApJ* 555, 685–708. [arXiv:astro-ph/0012213](#).
- Barthel, P.D., Tytler, D.R., Thomson, B., 1990. Optical spectra of distant radio loud quasars. I - Data: Spectra of 67 quasars. *A&ApS* 82, 339–389.
- Baskin, A., Laor, A., 2005. What controls the CIV line profile in active galactic nuclei? *MNRAS* 356, 1029–1044. [arXiv:astro-ph/0409196](#).
- Begelman, M.C., Hatchett, S.P., McKee, C.F., Sarazin, C.L., Arons, J., 1980. Beam models for SS 433. *ApJ* 238, 722–730.
- Bentz, M.C., Peterson, B.M., Pogge, R.W., Vestergaard, M., 2009. The Black Hole Mass-Bulge Luminosity Relationship for Active Galactic Nuclei From Reverberation Mapping and Hubble Space Telescope Imaging. *ApJL* 694, L166–L170. 0812.2284.
- Bentz, M.C., Peterson, B.M., Pogge, R.W., Vestergaard, M., Onken, C.A., 2006. The Radius-Luminosity Relationship for Active Galactic Nuclei: The Effect of Host-Galaxy Starlight on Luminosity Measurements. *ApJ* 644, 133–142. [arXiv:astro-ph/0602412](#).

- Bentz, M.C., Walsh, J.L., Barth, A.J., Yoshii, Y., Woo, J.H., Wang, X., Treu, T., Thornton, C.E., Street, R.A., Steele, T.N., Silverman, J.M., Serduke, F.J.D., Sakata, Y., Minezaki, T., Malkan, M.A., Li, W., Lee, N., Hiner, K.D., Hidas, M.G., Greene, J.E., Gates, E.L., Ganeshalingam, M., Filippenko, A.V., Canalizo, G., Bennert, V.N., Baliber, N., 2010. The Lick AGN Monitoring Project: Reverberation Mapping of Optical Hydrogen and Helium Recombination Lines. *ApJ* 716, 993–1011. 1004.2922.
- Bochkarev, N.G., Gaskell, C.M., 2009. The accuracy of supermassive black hole masses determined by the single-epoch spectrum (Dibai) method. *Astronomy Letters* 35, 287–293. 0809.4742.
- Bon, E., Popović, L.Č., Gavrilović, N., La Mura, G., Mediavilla, E., 2009. Contribution of a disc component to single-peaked broad lines of active galactic nuclei. *MNRAS* 400, 924–936. 0908.2939.
- Boroson, T.A., 2011. A New Orientation Indicator for Radio-quiet Quasars. *ApJL* 735, L14+. 1105.5161.
- Boroson, T.A., Lauer, T.R., 2009. A candidate sub-parsec supermassive binary black hole system. *Nature* 458, 53–55. 0901.3779.
- Botti, I., Lira, P., Netzer, H., Kaspi, S., 2010. High-Redshift Quasar Monitoring Campaign: Preliminary Results, in: *IAU Symposium*, pp. 198–198.
- Brotherton, M.S., Wills, B.J., Francis, P.J., Steidel, C.C., 1994. The intermediate line region of QSOs. *ApJ* 430, 495–504.
- Capetti, A., Marconi, A., Macchetto, D., Axon, D., 2005. The supermassive black hole in the Seyfert 2 galaxy NGC 5252. *AAp* 431, 465–475. [arXiv:astro-ph/0411081](#).
- Chao, L.H., Bian, W.H., Huang, K.L., 2008. The relation between the Black hole mass and the Bulge mass for low redshift AGNs. Part I: Ground-based observations. *Advances in Space Research* 42, 544–549.
- Cherepashchuk, A.M., Lyutyi, V.M., 1973. Rapid Variations of  $H\alpha$  Intensity in the Nuclei of Seyfert Galaxies NGC 4151, 3516, 1068. *ApL* 13, 165–+.
- Clavel, J., Reichert, G.A., Alloin, D., Crenshaw, D.M., Kriss, G., Krolik, J.H., Malkan, M.A., Netzer, H., Peterson, B.M., Wamsteker, W.,

- Altamore, A., Baribaud, T., Barr, P., Beck, S., Binette, L., Bromage, G.E., Brosch, N., Diaz, A.I., Filippenko, A.V., Fricke, K., Gaskell, C.M., Giommi, P., Glass, I.S., Gondhalekar, P., Hackney, R.L., Halpern, J.P., Hutter, D.J., Joersaeter, S., Kinney, A.L., Kollatschny, W., Koratkar, A., Korista, K.T., Laor, A., Lasota, J., Leibowitz, E., Maoz, D., Martin, P.G., Mazeh, T., Meurs, E.J.A., Nair, A.D., O’Brien, P., Pelat, D., Perez, E., Perola, G.C., Ptak, R.L., Rodriguez-Pascual, P., Rosenblatt, E.I., Sadun, A.C., Santos-Lleo, M., Shaw, R.A., Smith, P.S., Stirpe, G.M., Stoner, R., Sun, W.H., Ulrich, M., van Groningen, E., Zheng, W., 1991. Steps toward determination of the size and structure of the broad-line region in active galactic nuclei. I - an 8 month campaign of monitoring NGC 5548 with IUE. *ApJ* 366, 64–81.
- Collin, S., Kawaguchi, T., Peterson, B.M., Vestergaard, M., 2006. Systematic effects in measurement of black hole masses by emission-line reverberation of active galactic nuclei: Eddington ratio and inclination. *A&Ap* 456, 75–90. [arXiv:astro-ph/0603460](#).
- Crenshaw, D.M., Kraemer, S.B., Gabel, J.R., 2003. The Host Galaxies of Narrow-Line Seyfert 1 Galaxies: Evidence for Bar-Driven Fueling. *AJ* 126, 1690–1698. [arXiv:astro-ph/0306404](#).
- Croom, S.M., 2011. Do quasar broad-line velocity widths add any information to virial black hole mass estimates? *ArXiv e-prints* 1105.4391.
- Davidson, K., Netzer, H., 1979. The emission lines of quasars and similar objects. *Reviews of Modern Physics* 51, 715–766.
- De Robertis, M.M., Osterbrock, D.E., 1986. NGC 1320 - A feeble, high-ionization Seyfert 2 galaxy. *ApJ* 301, 98–104.
- Denney, K.D., Peterson, B.M., Pogge, R.W., Adair, A., Atlee, D.W., Au-Yong, K., Bentz, M.C., Bird, J.C., Brokofsky, D.J., Chisholm, E., Comins, M.L., Dietrich, M., Doroshenko, V.T., Eastman, J.D., Efimov, Y.S., Ewald, S., Ferbey, S., Gaskell, C.M., Hedrick, C.H., Jackson, K., Klimanov, S.A., Klimek, E.S., Kruse, A.K., Lad route, A., Lamb, J.B., Leighly, K., Minezaki, T., Nazarov, S.V., Onken, C.A., Petersen, E.A., Peterson, P., Poindexter, S., Sakata, Y., Schlesinger, K.J., Sergeev, S.G., Skolski, N., Stieglitz, L., Tobin, J.J., Unterborn, C., Vestergaard, M., Watkins, A.E., Watson, L.C., Yoshii, Y., 2010. Reverberation Mapping

- Measurements of Black Hole Masses in Six Local Seyfert Galaxies. *ApJ* 721, 715–737. 1006.4160.
- Dibai, E.A., 1977. Mass of the central bodies of active galaxy nuclei. *Soviet Astronomy Letters* 3, 1–3.
- Dibai, E.A., 1984. An Empirical Model for Active Galactic Nuclei - Part One - the Catalog. *SovA* 28, 245–+.
- Dietrich, M., Mathur, S., Grupe, D., Komossa, S., 2009. Black Hole Masses of Intermediate-Redshift Quasars: Near-Infrared Spectroscopy. *ApJ* 696, 1998–2013. 0901.3378.
- Edelson, R.A., Alexander, T., Crenshaw, D.M., Kaspi, S., Malkan, M.A., Peterson, B.M., Warwick, R.S., Clavel, J., Filippenko, A.V., Horne, K., Korista, K.T., Kriss, G.A., Krolik, J.H., Maoz, D., Nandra, K., O’Brien, P.T., Penton, S.V., Yaqoob, T., Albrecht, P., Alloin, D., Ayres, T.R., Balonek, T.J., Barr, P., Barth, A.J., Bertram, R., Bromage, G.E., Carini, M., Carone, T.E., Cheng, F.Z., Chuvaev, K.K., Dietrich, M., Dultzin-Hacyan, D., Gaskell, C.M., Glass, I.S., Goad, M.R., Hemar, S., Ho, L.C., Huchra, J.P., Hutchings, J., Johnson, W.N., Kazanas, D., Kollatschny, W., Koratkar, A.P., Kovo, O., Laor, A., MacAlpine, G.M., Magdziarz, P., Martin, P.G., Matheson, T., McCollum, B., Miller, H.R., Morris, S.L., Oknyanskij, V.L., Penfold, J., Perez, E., Perola, G.C., Pike, G., Pogge, R.W., Ptak, R.L., Qian, B.C., Recondo-Gonzalez, M.C., Reichert, G.A., Rodriguez-Espinoza, J.M., Rodriguez-Pascual, P.M., Rokaki, E.L., Roland, J., Sadun, A.C., Salamanca, I., Santos-Lleo, M., Shields, J.C., Shull, J.M., Smith, D.A., Smith, S.M., Snijders, M.A.J., Stirpe, G.M., Stoner, R.E., Sun, W.H., Ulrich, M.H., van Groningen, E., Wagner, R.M., Wagner, S., Wanders, I., Welsh, W.F., Weymann, R.J., Wilkes, B.J., Wu, H., Wurster, J., Xue, S.J., Zdziarski, A.A., Zheng, W., Zou, Z.L., 1996. Multiwavelength Observations of Short-Timescale Variability in NGC 4151. IV. Analysis of Multiwavelength Continuum Variability. *ApJ* 470, 364–+. [arXiv:astro-ph/9605082](#).
- Eracleous, M., Boroson, T.A., Halpern, J.P., Liu, J., 2011. A Large Systematic Search for Recoiling and Close Supermassive Binary Black Holes. *ArXiv e-prints* 1106.2952.

- Eracleous, M., Halpern, J.P., 2003. Completion of a Survey and Detailed Study of Double-peaked Emission Lines in Radio-loud Active Galactic Nuclei. *ApJ* 599, 886–908. [arXiv:astro-ph/0309149](#).
- Eracleous, M., Halpern, J.P., Gilbert, A.M., Newman, J.A., Filippenko, A.V., 1997. Rejection of the Binary Broad-Line Region Interpretation of Double-peaked Emission Lines in Three Active Galactic Nuclei. *ApJ* 490, 216–+. [arXiv:astro-ph/9706222](#).
- Fan, X., 2010. The Highest-Redshift Quasars, in: N. Kawai & S. Nagataki (Ed.), *American Institute of Physics Conference Series*, pp. 44–51.
- Ferland, G.J., Korista, K.T., Verner, D.A., Ferguson, J.W., Kingdon, J.B., Verner, E.M., 1998. CLOUDY 90: Numerical Simulation of Plasmas and Their Spectra. *PASP* 110, 761–778.
- Ferland, G.J., Peterson, B.M., Horne, K., Welsh, W.F., Nahar, S.N., 1992. Anisotropic line emission and the geometry of the broad-line region in active galactic nuclei. *ApJ* 387, 95–108.
- Ferrarese, L., Ford, H.C., Jaffe, W., 1996. Evidence for a Massive Black Hole in the Active Galaxy NGC 4261 from Hubble Space Telescope Images and Spectra. *ApJ* 470, 444–+.
- Ferrarese, L., Merritt, D., 2000. A Fundamental Relation between Supermassive Black Holes and Their Host Galaxies. *ApJL* 539, L9–L12. [arXiv:astro-ph/0006053](#).
- Gaskell, C.M., 1982. A redshift difference between high and low ionization emission-line regions in QSOs - Evidence for radial motions. *ApJ* 263, 79–86.
- Gaskell, C.M., 1983. Quasars as supermassive binaries, in: J.-P. Swings (Ed.), *Liege International Astrophysical Colloquia*, pp. 473–477.
- Gaskell, C.M., 1988. Direct evidence for gravitational domination of the motion of gas within one light-week of the central object in NGC 4151 and the determination of the mass of the probable black hole. *ApJ* 325, 114–118.

- Gaskell, C.M., 1996. Evidence for Binary Orbital Motion of a Quasar Broad-Line Region. *ApJL* 464, L107+. [arXiv:astro-ph/9605185](#).
- Gaskell, C.M., 2008. Accretion Disks and the Nature and Origin of AGN Continuum Variability, in: *Revista Mexicana de Astronomia y Astrofisica Conference Series*, pp. 1–11. [0711.2113](#).
- Gaskell, C.M., 2009a. An Improved [O III] Line Width to Stellar Velocity Dispersion Calibration: Curvature, Scatter, and Lack of Evolution in the Black-Hole Mass Versus Stellar Velocity Dispersion Relationship. *ArXiv e-prints* [0908.0328](#).
- Gaskell, C.M., 2009b. What broad emission lines tell us about how active galactic nuclei work. *NewARev* 53, 140–148. [0908.0386](#).
- Gaskell, C.M., 2010a. Accurate AGN Black Hole Masses and the Scatter in the  $M_{\text{BH}} - L_{\text{bulge}}$  Relationship, in: *IAU Symposium*, pp. 203–203. [1003.0036](#).
- Gaskell, C.M., 2010b. Close supermassive binary black holes. *Nature* 463. [0903.4447](#).
- Gaskell, C.M., 2010c. Off-Axis Energy Generation in Active Galactic Nuclei: Explaining Broad-Line Profiles, Spectropolarimetric Observations, and Velocity-Resolved Reverberation Mapping. *ArXiv e-prints* [1008.1057](#).
- Gaskell, C.M., Goosmann, R.W., 2008. Line Shifts, Broad-Line Region Inflow, and the Feeding of AGNs. *ArXiv e-prints* [0805.4258](#).
- Gaskell, C.M., Kormendy, J., 2009. An Improved Black Hole Mass-Bulge Luminosity Relationship for AGNs, in: S. Jogee, I. Marinova, L. Hao, & G. A. Blanc (Ed.), *Galaxy Evolution: Emerging Insights and Future Challenges*, pp. 388–+. [0907.1652](#).
- Gaskell, C.M., Sparke, L.S., 1986. Line variations in quasars and Seyfert galaxies. *ApJ* 305, 175–186.
- Gebhardt, K., Bender, R., Bower, G., Dressler, A., Faber, S.M., Filippenko, A.V., Green, R., Grillmair, C., Ho, L.C., Kormendy, J., Lauer, T.R., Magorrian, J., Pinkney, J., Richstone, D., Tremaine, S., 2000. A Relationship between Nuclear Black Hole Mass and Galaxy Velocity Dispersion. *ApJL* 539, L13–L16. [arXiv:astro-ph/0006289](#).



- Gezari, S., Halpern, J.P., Eracleous, M., 2007. Long-Term Profile Variability of Double-peaked Emission Lines in Active Galactic Nuclei. *ApJS* 169, 167–212. [arXiv:astro-ph/0702594](#).
- Graham, A.W., Onken, C.A., Athanassoula, E., Combes, F., 2011. An expanded  $M_{\text{bh}}\text{-}\sigma$  diagram, and a new calibration of active galactic nuclei masses. *MNRAS* 412, 2211–2228. [1007.3834](#).
- Greene, J.E., Hood, C.E., Barth, A.J., Bennert, V.N., Bentz, M.C., Filippenko, A.V., Gates, E., Malkan, M.A., Treu, T., Walsh, J.L., Woo, J.H., 2010a. The Lick AGN Monitoring Project: Alternate Routes to a Broad-line Region Radius. *ApJ* 723, 409–416. [1009.0532](#).
- Greene, J.E., Peng, C.Y., Kim, M., Kuo, C.Y., Braatz, J.A., Violette Impellizzeri, C.M., Condon, J.J., Lo, K.Y., Henkel, C., Reid, M.J., 2010b. Precise Black Hole Masses from Megamaser Disks: Black Hole-Bulge Relations at Low Mass. *ApJ* 721, 26–45. [1007.2851](#).
- Greenstein, J.L., Schmidt, M., 1964. The Quasi-Stellar Radio Sources 3c 48 and 3c 273. *ApJ* 140, 1–+.
- Gültekin, K., Richstone, D.O., Gebhardt, K., Lauer, T.R., Tremaine, S., Aller, M.C., Bender, R., Dressler, A., Faber, S.M., Filippenko, A.V., Green, R., Ho, L.C., Kormendy, J., Magorrian, J., Pinkney, J., Siopis, C., 2009. The  $M\text{-}\sigma$  and  $M\text{-}L$  Relations in Galactic Bulges, and Determinations of Their Intrinsic Scatter. *ApJ* 698, 198–221. [0903.4897](#).
- Gültekin, K., Tremaine, S., Loeb, A., Richstone, D.O., 2011. Observational selection effects and the  $M\text{-}\sigma$  relation. *ArXiv e-prints* [1106.1079](#).
- Halpern, J.P., Filippenko, A.V., 1988. A test of the massive binary black hole hypothesis - ARP 102B. *Nature* 331, 46–48.
- Hayashida, K., Miyamoto, S., Kitamoto, S., Negoro, H., Inoue, H., 1998. Central Black Hole Masses in Active Galactic Nuclei Inferred from X-Ray Variability. *ApJ* 500, 642–+.
- Horne, K., Peterson, B.M., Collier, S.J., Netzer, H., 2004. Observational Requirements for High-Fidelity Reverberation Mapping. *PASP* 116, 465–476.

- Hoyle, F., Fowler, W.A., 1963. Nature of Strong Radio Sources. *Nature* 197, 533–535.
- Hu, C., Wang, J.M., Ho, L.C., Chen, Y.M., Zhang, H.T., Bian, W.H., Xue, S.J., 2008. A Systematic Analysis of Fe II Emission in Quasars: Evidence for Inflow to the Central Black Hole. *ApJ* 687, 78–96. 0807.2059.
- Jarvis, M.J., McLure, R.J., 2006. Orientation dependency of broad-line widths in quasars and consequences for black hole mass estimation. *MNRAS* 369, 182–188. [arXiv:astro-ph/0603231](#).
- Jovanović, P., Popović, L.Č., Stalevski, M., Shapovalova, A.I., 2010. Variability of the  $H\beta$  Line Profiles as an Indicator of Orbiting Bright Spots in Accretion Disks of Quasars: A Case Study of 3C 390.3. *ApJ* 718, 168–176. 1005.5039.
- Kallman, T.R., Krolik, J.H., 1986. The effects of electron scattering opacity in the broad emission-line regions of quasars. *ApJ* 308, 805–814.
- Kaspi, S., Brandt, W.N., Maoz, D., Netzer, H., Schneider, D.P., Shemmer, O., 2007. Reverberation Mapping of High-Luminosity Quasars: First Results. *ApJ* 659, 997–1007. [arXiv:astro-ph/0612722](#).
- Kaspi, S., Maoz, D., Netzer, H., Peterson, B.M., Vestergaard, M., Jannuzi, B.T., 2005. The Relationship between Luminosity and Broad-Line Region Size in Active Galactic Nuclei. *ApJ* 629, 61–71. [arXiv:astro-ph/0504484](#).
- Kaspi, S., Smith, P.S., Netzer, H., Maoz, D., Jannuzi, B.T., Giveon, U., 2000. Reverberation Measurements for 17 Quasars and the Size-Mass-Luminosity Relations in Active Galactic Nuclei. *ApJ* 533, 631–649. [arXiv:astro-ph/9911476](#).
- Klimek, E.S., Gaskell, C.M., Hedrick, C.H., 2004. Optical Variability of Narrow-Line Seyfert 1 Galaxies. *ApJ* 609, 69–79. [arXiv:astro-ph/0403334](#).
- Komossa, S., Xu, D., 2007. Narrow-Line Seyfert 1 Galaxies and the  $M_{\text{BH}}-\sigma$  Relation. *ApJL* 667, L33–L36. 0708.0256.
- Koratkar, A.P., Gaskell, C.M., 1989. Emission-line variability of Fairall 9 - Determination of the size of the broad-line region and the direction of gas motion. *ApJ* 345, 637–646.

- Koratkar, A.P., Gaskell, C.M., 1991. Structure and kinematics of the broad-line regions in active galaxies from IUE variability data. *ApJS* 75, 719–750.
- Korista, K., Baldwin, J., Ferland, G., Verner, D., 1997. An Atlas of Computed Equivalent Widths of Quasar Broad Emission Lines. *ApJS* 108, 401–+. [arXiv:astro-ph/9611220](#).
- Korista, K.T., Alloin, D., Barr, P., Clavel, J., Cohen, R.D., Crenshaw, D.M., Evans, I.N., Horne, K., Koratkar, A.P., Kriss, G.A., Krolik, J.H., Malkan, M.A., Morris, S.L., Netzer, H., O’Brien, P.T., Peterson, B.M., Reichert, G.A., Rodriguez-Pascual, P.M., Wamsteker, W., Anderson, K.S.J., Axon, D.J., Benitez, E., Berlind, P., Bertram, R., Blackwell, Jr., J.H., Bochkarev, N.G., Boisson, C., Carini, M., Carrillo, R., Carone, T.E., Cheng, F.Z., Christensen, J.A., Chuvaev, K.K., Dietrich, M., Dokter, J.J., Doroshenko, V., Dultzin-Hacyan, D., England, M.N., Espey, B.R., Filippenko, A.V., Gaskell, C.M., Goad, M.R., Ho, L.C., Huchra, J.P., Jiang, X.J., Kaspi, S., Kollatschny, W., Laor, A., Luminet, J.P., MacAlpine, G.M., MacKenty, J.W., Malkov, Y.F., Maoz, D., Martin, P.G., Matheson, T., McCollum, B., Merkulova, N., Metik, L., Mignoli, M., Miller, H.R., Pastoriza, M.G., Pelat, D., Penfold, J., Perez, M., Perola, G.C., Persaud, J.L., Peters, J., Pitts, R., Pogge, R.W., Pronik, I., Pronik, V.I., Ptak, R.L., Rawley, L., Recondo-Gonzalez, M.C., Rodriguez-Espinosa, J.M., Romanishin, W., Sadun, A.C., Salamanca, I., Santos-Lleo, M., Sekiguchi, K., Sergeev, S.G., Shapovalova, A.I., Shields, J.C., Shrader, C., Shull, J.M., Silbermann, N.A., Sitko, M.L., Skillman, D.R., Smith, H.A., Smith, S.M., Snijders, M.A.J., Sparke, L.S., Stirpe, G.M., Stoner, R.E., Sun, W.H., Thiele, U., Tokarz, S., Tsvetanov, Z.I., Turnshek, D.A., Veilleux, S., Wagner, R.M., Wagner, S.J., Wanders, I., Wang, T., Welsh, W.F., Weymann, R.J., White, R.J., Wilkes, B.J., Wills, B.J., Winge, C., Wu, H., Zou, Z.L., 1995. Steps toward determination of the size and structure of the broad-line region in active galactic nuclei. 8: an intensive HST, IUE, and ground-based study of NGC 5548. *ApJS* 97, 285–330.
- Korista, K.T., Goad, M.R., 2004. What the Optical Recombination Lines Can Tell Us about the Broad-Line Regions of Active Galactic Nuclei. *ApJ* 606, 749–762. [arXiv:astro-ph/0402506](#).

- Kormendy, J., 1993. A critical review of stellar-dynamical evidence for black holes in galaxy nuclei, in: J. Beckman, L. Colina, & H. Netzer (Ed.), *The Nearest Active Galaxies*, pp. 197–218.
- Kormendy, J., Richstone, D., 1995. Inward Bound—The Search For Super-massive Black Holes In Galactic Nuclei. *ARAAp* 33, 581–+.
- Kovačević, J., Popović, L.Č., Dimitrijević, M.S., 2010. Analysis of Optical Fe II Emission in a Sample of Active Galactic Nucleus Spectra. *ApJS* 189, 15–36. 1004.2212.
- Krolik, J.H., 2001. Systematic Errors in the Estimation of Black Hole Masses by Reverberation Mapping. *ApJ* 551, 72–79. [arXiv:astro-ph/0012134](#).
- Krongold, Y., Dultzin-Hacyan, D., Marziani, P., 2001. Host Galaxies and Circumgalactic Environment of “Narrow Line” Seyfert 1 Nuclei. *AJ* 121, 702–709.
- Kuo, C.Y., Braatz, J.A., Condon, J.J., Impellizzeri, C.M.V., Lo, K.Y., Zaw, I., Schenker, M., Henkel, C., Reid, M.J., Greene, J.E., 2011. The Megamaser Cosmology Project. III. Accurate Masses of Seven Supermassive Black Holes in Active Galaxies with Circumnuclear Megamaser Disks. *ApJ* 727, 20–+. 1008.2146.
- Kurk, J.D., Walter, F., Fan, X., Jiang, L., Riechers, D.A., Rix, H.W., Pentericci, L., Strauss, M.A., Carilli, C., Wagner, S., 2007. Black Hole Masses and Enrichment of  $z \sim 6$  SDSS Quasars. *ApJ* 669, 32–44. 0707.1662.
- Labita, M., Decarli, R., Treves, A., Falomo, R., 2009. Downsizing of super-massive black holes from the SDSS quasar survey - II. Extension to  $z \sim 4$ . *MNRAS* 399, 2099–2106. 0907.2963.
- Laor, A., 2001. On the Linearity of the Black Hole-Bulge Mass Relation in Active and in Nearby Galaxies. *ApJ* 553, 677–682. [arXiv:astro-ph/0101405](#).
- Lewis, K.T., Eracleous, M., 2006. Black Hole Masses of Active Galaxies with Double-peaked Balmer Emission Lines. *ApJ* 642, 711–719. [arXiv:astro-ph/0601398](#).

- Lyutyi, V.M., Cherepashchuk, A.M., 1972. *Astronomicheskij Tsirkulyar* 688, 1–+.
- Macchetto, F., Marconi, A., Axon, D.J., Capetti, A., Sparks, W., Crane, P., 1997. The Supermassive Black Hole of M87 and the Kinematics of Its Associated Gaseous Disk. *ApJ* 489, 579–+. [arXiv:astro-ph/9706252](#).
- Magorrian, J., Tremaine, S., Richstone, D., Bender, R., Bower, G., Dressler, A., Faber, S.M., Gebhardt, K., Green, R., Grillmair, C., Kormendy, J., Lauer, T., 1998. The Demography of Massive Dark Objects in Galaxy Centers. *AJ* 115, 2285–2305. [arXiv:astro-ph/9708072](#).
- Mainieri, V., Rigopoulou, D., Lehmann, I., Scott, S., Matute, I., Almaini, O., Tozzi, P., Hasinger, G., Dunlop, J.S., 2005. Submillimetre detection of a high-redshift type 2 QSO. *MNRAS* 356, 1571–1575. [arXiv:astro-ph/0410632](#).
- Marconi, A., Axon, D.J., Maiolino, R., Nagao, T., Pastorini, G., Pietrini, P., Robinson, A., Torricelli, G., 2008. The Effect of Radiation Pressure on Virial Black Hole Mass Estimates and the Case of Narrow-Line Seyfert 1 Galaxies. *ApJ* 678, 693–700. 0802.2021.
- Marconi, A., Axon, D.J., Maiolino, R., Nagao, T., Pietrini, P., Risaliti, G., Robinson, A., Torricelli, G., 2009. On the Observed Distributions of Black Hole Masses and Eddington Ratios from Radiation Pressure Corrected Virial Indicators. *ApJL* 698, L103–L107. 0905.0539.
- Marconi, A., Hunt, L.K., 2003. The Relation between Black Hole Mass, Bulge Mass, and Near-Infrared Luminosity. *ApJL* 589, L21–L24. [arXiv:astro-ph/0304274](#).
- Marziani, P., Dultzin-Hacyan, D., Sulentic, J.W., 2006. Accretion onto Supermassive Black Holes in Quasars: Learning from Optical/UV Observations. *New Developments in Black Hole Research*. p. 123.
- Marziani, P., Sulentic, J.W., Dultzin-Hacyan, D., Calvani, M., Moles, M., 1996. Comparative Analysis of the High- and Low-Ionization Lines in the Broad-Line Region of Active Galactic Nuclei. *ApJS* 104, 37–+.

- Marziani, P., Sulentic, J.W., Negrete, C.A., Dultzin, D., Zamfir, S., Bachev, R., 2010. Broad-line region physical conditions along the quasar eigenvector 1 sequence. *MNRAS* 409, 1033–1048. 1007.3187.
- Marziani, P., Sulentic, J.W., Stirpe, G.M., Zamfir, S., Calvani, M., 2009. VLT/ISAAC spectra of the  $H\beta$  region in intermediate-redshift quasars. III.  $H\beta$  broad-line profile analysis and inferences about BLR structure. *A&Ap* 495, 83–112. 0812.0251.
- Marziani, P., Sulentic, J.W., Zamanov, R., Calvani, M., Dultzin-Hacyan, D., Bachev, R., Zwitter, T., 2003a. An Optical Spectroscopic Atlas of Low-Redshift Active Galactic Nuclei. *ApJS* 145, 199–211.
- Marziani, P., Zamanov, R.K., Sulentic, J.W., Calvani, M., 2003b. Searching for the physical drivers of eigenvector 1: influence of black hole mass and Eddington ratio. *MNRAS* 345, 1133–1144. [arXiv:astro-ph/0307367](#).
- Mathis, J.S., 1970. Electron Scattering in Seyfert Galaxies. *ApJ* 162, 761–+.
- Mathur, S., Kuraszkiewicz, J., Czerny, B., 2001. Evolution of active galaxies: black-hole mass-bulge relations for narrow line objects. *NewA* 6, 321–329. [arXiv:astro-ph/0104263](#).
- McLure, R.J., Dunlop, J.S., 2004. The cosmological evolution of quasar black hole masses. *MNRAS* 352, 1390–1404. [arXiv:astro-ph/0310267](#).
- McLure, R.J., Jarvis, M.J., 2002. Measuring the black hole masses of high-redshift quasars. *MNRAS* 337, 109–116. [arXiv:astro-ph/0204473](#).
- Meadows, Z., Zamfir, S., Marziani, P., Sulentic, J.W., 2011. Modeling the  $H\beta$  Emission Lines in Luminosity-Averaged Quasar Spectra, in: American Astronomical Society Meeting Abstracts #218, pp. # 327.12–+.
- Merritt, D., Ferrarese, L., 2001. The  $M_*$ - $\sigma$  Relation for Supermassive Black Holes. *ApJ* 547, 140–145. [arXiv:astro-ph/0008310](#).
- Miley, G.K., Miller, J.S., 1979. Relations between the emission spectra and radio structures of quasars. *ApJL* 228, L55–L58.
- Miyoshi, M., Moran, J., Herrnstein, J., Greenhill, L., Nakai, N., Diamond, P., Inoue, M., 1995. Evidence for a black hole from high rotation velocities in a sub-parsec region of NGC4258. *Nature* 373, 127–129.

- Moorwood, A., Cuby, J.G., Biereichel, P., Brynnel, J., Delabre, B., Devillard, N., van Dijsseldonk, A., Finger, G., Gemperlein, H., Gilmozzi, R., Herlin, T., Huster, G., Knudstrup, J., Lidman, C., Lizon, J.L., Mehrgan, H., Meyer, M., Nicolini, G., Petr, M., Spyromilio, J., Stegmeier, J., 1998. ISAAC sees first light at the VLT. *The Messenger* 94, 7–9.
- Mortlock, D.J., Warren, S.J., Venemans, B.P., Patel, M., Hewett, P.C., McMahon, R.G., Simpson, C., Theuns, T., González-Solares, E.A., Adamson, A., Dye, S., Hambly, N.C., Hirst, P., Irwin, M.J., Kuiper, E., Lawrence, A., Röttgering, H.J.A., 2011. A luminous quasar at a redshift of  $z = 7.085$ . *Nature* 474, 616–619. [1106.6088](#).
- Nagao, T., Marconi, A., Maiolino, R., 2006. The evolution of the broad-line region among SDSS quasars. *A&Ap* 447, 157–172. [arXiv:astro-ph/0510385](#).
- Negrete, C.A., 2011. ESTUDIO ESTRUCTURAL DE LA REGIÓN DE LÍNEAS ANCHAS EN CUASARES. Ph.D. thesis. UNAM, Mexico, (2001).
- Negrete, C.A., Dultzin, D., Marziani, P., Sulentic, J., 2010. Physical Conditions in the Broad Line Region of  $\sim 3\%$  Quasars: A Photoionization Method to Derive  $f_{\text{BLR}}$ . *ArXiv e-prints* 1011.4248.
- Nelson, C.H., 2000. Black Hole Mass, Velocity Dispersion, and the Radio Source in Active Galactic Nuclei. *ApJL* 544, L91–L94. [arXiv:astro-ph/0009188](#).
- Nelson, C.H., Green, R.F., Bower, G., Gebhardt, K., Weistrop, D., 2004. The Relationship Between Black Hole Mass and Velocity Dispersion in Seyfert 1 Galaxies. *ApJ* 615, 652–661. [arXiv:astro-ph/0407383](#).
- Netzer, H., 2003. The Largest Black Holes and the Most Luminous Galaxies. *ApJL* 583, L5–L8. [arXiv:astro-ph/0210548](#).
- Netzer, H., Lira, P., Trakhtenbrot, B., Shemmer, O., Cury, I., 2007. Black Hole Mass and Growth Rate at High Redshift. *ApJ* 671, 1256–1263. [0708.3787](#).

- Netzer, H., Marziani, P., 2010. The Effect of Radiation Pressure on Emission-line Profiles and Black Hole Mass Determination in Active Galactic Nuclei. *ApJ* 724, 318–328. 1006.3553.
- Netzer, H., Shemmer, O., Maiolino, R., Oliva, E., Croom, S., Corbett, E., di Fabrizio, L., 2004. Near-Infrared Spectroscopy of High-Redshift Active Galactic Nuclei. II. Disappearing Narrow-Line Regions and the Role of Accretion. *ApJ* 614, 558–567. [arXiv:astro-ph/0406560](#).
- Newman, J.A., Eracleous, M., Filippenko, A.V., Halpern, J.P., 1997. Measurement of an Active Galactic Nucleus Central Mass on Centiparsec Scales: Results of Long-Term Optical Monitoring of ARP 102B. *ApJ* 485, 570–+. [arXiv:astro-ph/9703023](#).
- Nikolajuk, M., Papadakis, I.E., Czerny, B., 2004. Black hole mass estimation from X-ray variability measurements in active galactic nuclei. *MNRAS* 350, L26–L30. [arXiv:astro-ph/0403326](#).
- Ohta, K., Aoki, K., Kawaguchi, T., Kiuchi, G., 2007. A Bar Fuels a Supermassive Black Hole?: Host Galaxies of Narrow-Line Seyfert 1 Galaxies. *ApJS* 169, 1–20. [arXiv:astro-ph/0610355](#).
- Onken, C.A., Ferrarese, L., Merritt, D., Peterson, B.M., Pogge, R.W., Vestergaard, M., Wandel, A., 2004. Supermassive Black Holes in Active Galactic Nuclei. II. Calibration of the Black Hole Mass-Velocity Dispersion Relationship for Active Galactic Nuclei. *ApJ* 615, 645–651. [arXiv:astro-ph/0407297](#).
- Padovani, P., 1989. The evolution of the Eddington ratio for active galactic nuclei. *AAp* 209, 27–45.
- Padovani, P., Burg, R., Edelson, R.A., 1990. The mass function of Seyfert 1 nuclei. *ApJ* 353, 438–444.
- Padovani, P., Rafanelli, P., 1988. Mass-luminosity relationships and accretion rates for Seyfert 1 galaxies and quasars. *AAp* 205, 53–70.
- Peterson, B.M., 1993. Reverberation mapping of active galactic nuclei. *PASP* 105, 247–268.



- Peterson, B.M., 2008. The central black hole and relationships with the host galaxy. *NewARev* 52, 240–252.
- Peterson, B.M., Balonek, T.J., Barker, E.S., Bechtold, J., Bertram, R., Bochkarev, N.G., Bolte, M.J., Bond, D., Boroson, T.A., Carini, M.T., Carone, T.E., Christensen, J.A., Clements, S.D., Cochran, A.L., Cohen, R.D., Crampton, D., Dietrich, M., Elvis, M., Ferguson, A., Filippenko, A.V., Fricke, K.J., Gaskell, C.M., Halpern, J.P., Huchra, J.P., Hutchings, J.B., Kollatschny, W., Koratkar, A.P., Korista, K.T., Krolik, J.H., Lam, N.J., Laor, A., Leacock, R.J., MacAlpine, G.M., Malkan, M.A., Maoz, D., Miller, H.R., Morris, S.L., Netzer, H., Oliveira, C.L.M., Penfold, J., Penston, M.V., Perez, E., Pogge, R.W., Richmond, M.W., Romanishin, W., Rosenblatt, E.I., Saddlemyer, L., Sadun, A., Sawyer, S.R., Shields, J.C., Shapovalova, A.I., Smith, A.G., Smith, H.A., Smith, P.S., Sun, W.H., Thiele, U., Turner, T.J., Veilleux, S., Wagner, R.M., Weymann, R.J., Wilkes, B.J., Wills, B.J., Wills, D., Younger, P.F., 1991. Steps toward determination of the size and structure of the broad-line region in active galactic nuclei. II - an intensive study of NGC 5548 at optical wavelengths. *ApJ* 368, 119–137.
- Peterson, B.M., Berlind, P., Bertram, R., Bischoff, K., Bochkarev, N.G., Borisov, N., Burenkov, A.N., Calkins, M., Carrasco, L., Chavushyan, V.H., Chornock, R., Dietrich, M., Doroshenko, V.T., Ezhkova, O.V., Filippenko, A.V., Gilbert, A.M., Huchra, J.P., Kollatschny, W., Leonard, D.C., Li, W., Lyuty, V.M., Malkov, Y.F., Matheson, T., Merkulova, N.I., Mikhailov, V.P., Modjaz, M., Onken, C.A., Pogge, R.W., Pronik, V.I., Qian, B., Romano, P., Sergeev, S.G., Sergeeva, E.A., Shapovalova, A.I., Spiridonova, O.I., Tao, J., Tokarz, S., Valdes, J.R., Vlasuk, V.V., Wagner, R.M., Wilkes, B.J., 2002. Steps toward Determination of the Size and Structure of the Broad-Line Region in Active Galactic Nuclei. XVI. A 13 Year Study of Spectral Variability in NGC 5548. *ApJ* 581, 197–204. [arXiv:astro-ph/0208064](#).
- Peterson, B.M., Ferrarese, L., Gilbert, K.M., Kaspi, S., Malkan, M.A., Maoz, D., Merritt, D., Netzer, H., Onken, C.A., Pogge, R.W., Vestergaard, M., Wandel, A., 2004. Central Masses and Broad-Line Region Sizes of Active Galactic Nuclei. II. A Homogeneous Analysis of a Large Reverberation-Mapping Database. *ApJ* 613, 682–699. [arXiv:astro-ph/0407299](#).

- Peterson, B.M., Horne, K., 2006. Reverberation mapping of active galactic nuclei, in: M. Livio & S. Casertano (Ed.), *Planets to Cosmology: Essential Science in the Final Years of the Hubble Space Telescope*, pp. 89–+.
- Peterson, B.M., Wandel, A., 1999. Keplerian Motion of Broad-Line Region Gas as Evidence for Supermassive Black Holes in Active Galactic Nuclei. *ApJL* 521, L95–L98. [arXiv:astro-ph/9905382](#).
- Pronik, V.I., Chuvaev, K.K., 1972. Hydrogen lines in the spectrum of the galaxy Markaryan 6 during its activity. *Astrophysics* 8, 112–116.
- Rafiee, A., Hall, P.B., 2011. Supermassive Black Hole Mass Estimates Using Sloan Digital Sky Survey Quasar Spectra at  $0.7 < z < 2$ . *ApJS* 194, 42–+. 1104.1828.
- Richards, G.T., Kruczek, N.E., Gallagher, S.C., Hall, P.B., Hewett, P.C., Leighly, K.M., Deo, R.P., Kratzer, R.M., Shen, Y., 2011. Unification of Luminous Type 1 Quasars through C IV Emission. *AJ* 141, 167–+. 1011.2282.
- Rokaki, E., Lawrence, A., Economou, F., Mastichiadis, A., 2003. Is there a disc in the superluminal quasars? *MNRAS* 340, 1298–1308. [arXiv:astro-ph/0301405](#).
- Salpeter, E.E., 1964. Accretion of Interstellar Matter by Massive Objects. *ApJ* 140, 796–800.
- Salviander, S., Shields, G.A., Gebhardt, K., Bonning, E.W., 2007. The Black Hole Mass-Galaxy Bulge Relationship for QSOs in the Sloan Digital Sky Survey Data Release 3. *ApJ* 662, 131–144. [arXiv:astro-ph/0612568](#).
- Schneider, D.P., Fan, X., Hall, P.B., Jester, S., Richards, G.T., Stoughton, C., Strauss, M.A., SubbaRao, M., Vanden Berk, D.E., Anderson, S.F., Brandt, W.N., Gunn, J.E., Gray, J., Trump, J.R., Voges, W., Yanny, B., Bahcall, N.A., Blanton, M.R., Boroski, W.N., Brinkmann, J., Brunner, R., Burles, S., Castander, F.J., Doi, M., Eisenstein, D., Frieman, J.A., Fukugita, M., Heckman, T.M., Hennessy, G.S., Ivezić, Ž., Kent, S., Knapp, G.R., Lamb, D.Q., Lee, B.C., Loveday, J., Lupton, R.H., Margon, B., Meiksin, A., Munn, J.A., Newberg, H.J., Nichol, R.C., Niederste-Ostholt, M., Pier, J.R., Richmond, M.W., Rockosi, C.M., Saxe, D.H., Schlegel,

- D.J., Szalay, A.S., Thakar, A.R., Uomoto, A., York, D.G., 2003. The Sloan Digital Sky Survey Quasar Catalog. II. First Data Release. *AJ* 126, 2579–2593. [arXiv:astro-ph/0308443](#).
- Severgnini, P., Caccianiga, A., Braito, V., Della Ceca, R., Maccacaro, T., Akiyama, M., Carrera, F.J., Ceballos, M.T., Page, M.J., Saracco, P., Watson, M.G., 2006. An X-ray bright ERO hosting a type 2 QSO. *AAp* 451, 859–864. [arXiv:astro-ph/0602486](#).
- Shapiro, K.L., Cappellari, M., de Zeeuw, T., McDermid, R.M., Gebhardt, K., van den Bosch, R.C.E., Statler, T.S., 2006. The black hole in NGC 3379: a comparison of gas and stellar dynamical mass measurements with HST and integral-field data. *MNRAS* 370, 559–579. [arXiv:astro-ph/0605479](#).
- Shapovalova, A.I., Burenkov, A.N., Carrasco, L., Chavushyan, V.H., Doroshenko, V.T., Dumont, A.M., Lyuty, V.M., Valdés, J.R., Vlasuyk, V.V., Bochkarev, N.G., Collin, S., Legrand, F., Mikhailov, V.P., Spiridonova, O.I., Kurtanidze, O., Nikolashvili, M.G., 2001. Intermediate resolution  $H\beta$  spectroscopy and photometric monitoring of 3C 390.3. I. Further evidence of a nuclear accretion disk. *AAp* 376, 775–792. [arXiv:astro-ph/0106423](#).
- Shemmer, O., Netzer, H., Maiolino, R., Oliva, E., Croom, S., Corbett, E., di Fabrizio, L., 2004. Near-Infrared Spectroscopy of High-Redshift Active Galactic Nuclei. I. A Metallicity-Accretion Rate Relationship. *ApJ* 614, 547–557. [arXiv:astro-ph/0406559](#).
- Shen, Y., Greene, J.E., Strauss, M.A., Richards, G.T., Schneider, D.P., 2008. Biases in Virial Black Hole Masses: An SDSS Perspective. *ApJ* 680, 169–190. 0709.3098.
- Shen, Y., Loeb, A., 2010. Identifying Supermassive Black Hole Binaries with Broad Emission Line Diagnosis. *ApJ* 725, 249–260. 0912.0541.
- Shields, G.A., Gebhardt, K., Salviander, S., Wills, B.J., Xie, B., Brotherton, M.S., Yuan, J., Dietrich, M., 2003. The Black Hole-Bulge Relationship in Quasars. *ApJ* 583, 124–133. [arXiv:astro-ph/0210050](#).
- Smith, H.J., Hoeffeit, D., 1965. Light Variations in the Super-luminous Radio Galaxy 3C 273, in: I. Robinson, A. Schild, & E. L. Schucking (Ed.), *Quasi-Stellar Sources and Gravitational Collapse*, pp. 461–+.

- Storchi-Bergmann, T., Nemmen da Silva, R., Eracleous, M., Halpern, J.P., Wilson, A.S., Filippenko, A.V., Ruiz, M.T., Smith, R.C., Nagar, N.M., 2003. Evolution of the Nuclear Accretion Disk Emission in NGC 1097: Getting Closer to the Black Hole. *ApJ* 598, 956–968. [arXiv:astro-ph/0308327](#).
- Strateva, I.V., Strauss, M.A., Hao, L., Schlegel, D.J., Hall, P.B., Gunn, J.E., Li, L., Ivezić, Ž., Richards, G.T., Zakamska, N.L., Voges, W., Anderson, S.F., Lupton, R.H., Schneider, D.P., Brinkmann, J., Nichol, R.C., 2003. Double-peaked Low-Ionization Emission Lines in Active Galactic Nuclei. *AJ* 126, 1720–1749. [arXiv:astro-ph/0307357](#).
- Sulentic, J.W., Bachev, R., Marziani, P., Negrete, C.A., Dultzin, D., 2007. C IV  $\lambda 1549$  as an Eigenvector 1 Parameter for Active Galactic Nuclei. *ApJ* 666, 757–777. 0705.1895.
- Sulentic, J.W., Marziani, P., 1999. The Intermediate-Line Region in Active Galactic Nuclei: A Region “Præter Necessitatem”? *ApJL* 518, L9–L12. [arXiv:astro-ph/9904203](#).
- Sulentic, J.W., Marziani, P., Dultzin-Hacyan, D., 2000a. Phenomenology of Broad Emission Lines in Active Galactic Nuclei. *ARA&A* 38, 521–571.
- Sulentic, J.W., Marziani, P., Zamanov, R., Bachev, R., Calvani, M., Dultzin-Hacyan, D., 2002. Average Quasar Spectra in the Context of Eigenvector 1. *ApJL* 566, L71–L75. [arXiv:astro-ph/0201362](#).
- Sulentic, J.W., Repetto, P., Stirpe, G.M., Marziani, P., Dultzin-Hacyan, D., Calvani, M., 2006. VLT/ISAAC spectra of the  $H\beta$  region in intermediate-redshift quasars. II. Black hole mass and Eddington ratio. *A&Ap* 456, 929–939. [arXiv:astro-ph/0606309](#).
- Sulentic, J.W., Zamfir, S., Marziani, P., Bachev, R., Calvani, M., Dultzin-Hacyan, D., 2003. Radio-loud Active Galactic Nuclei in the Context of the Eigenvector 1 Parameter Space. *ApJL* 597, L17–L20. [arXiv:astro-ph/0309469](#).
- Sulentic, J.W., Zwitter, T., Marziani, P., Dultzin-Hacyan, D., 2000b. Eigenvector 1: An Optimal Correlation Space for Active Galactic Nuclei. *ApJL* 536, L5–L9. [arXiv:astro-ph/0005177](#).

- Targett, T.A., Dunlop, J.S., McLure, R.J., 2011. The host galaxies and black-hole:galaxy mass ratios of luminous quasars at  $z \sim 4$ . ArXiv e-prints 1107.2397.
- Trakhtenbrot, B., Netzer, H., Lira, P., Shemmer, O., 2011. Black Hole Mass and Growth Rate at  $z \sim 4.8$ : A Short Episode of Fast Growth Followed by Short Duty Cycle Activity. ApJ 730, 7–+. 1012.1871.
- Trevese, D., Paris, D., Stirpe, G.M., Vagnetti, F., Zitelli, V., 2007. Line and continuum variability of two intermediate-redshift, high-luminosity quasars. AAp 470, 491–496. 0704.1958.
- Tsalmantza, P., Decarli, R., Dotti, M., Hogg, D.W., 2011. A systematic search for massive black hole binaries in SDSS spectroscopic sample. ArXiv e-prints 1106.1180.
- Turler, M., Courvoisier, T.J.L., 1998. Principal component analysis of two ultraviolet emission-lines in 18 active galactic nuclei. AAp 329, 863–872. arXiv:astro-ph/9709038.
- Véron-Cetty, M.P., Véron, P., Gonçalves, A.C., 2001. A spectrophotometric atlas of Narrow-Line Seyfert 1 galaxies. AAp 372, 730–754. arXiv:astro-ph/0104151.
- Vestergaard, M., 2002. Determining Central Black Hole Masses in Distant Active Galaxies. ApJ 571, 733–752. arXiv:astro-ph/0204106.
- Vestergaard, M., Peterson, B.M., 2006. Determining Central Black Hole Masses in Distant Active Galaxies and Quasars. II. Improved Optical and UV Scaling Relationships. ApJ 641, 689–709. arXiv:astro-ph/0601303.
- Volonteri, M., Miller, J.M., Dotti, M., 2009. Sub-Parsec Supermassive Binary Quasars: Expectations at  $z < 1$ . ApJL 703, L86–L89. 0903.3947.
- Wandel, A., Peterson, B.M., Malkan, M.A., 1999. Central Masses and Broad-Line Region Sizes of Active Galactic Nuclei. I. Comparing the Photoionization and Reverberation Techniques. ApJ 526, 579–591. arXiv:astro-ph/9905224.
- Wandel, A., Yahil, A., 1985. Universal mass-luminosity relation for quasars and active galactic nuclei? ApJL 295, L1–L4.

- Wang, J., Dong, X., Wang, T., Ho, L.C., Yuan, W., Wang, H., Zhang, K., Zhang, S., Zhou, H., 2009. Estimating Black Hole Masses in Active Galactic Nuclei Using the Mg II  $\lambda$ 2800 Emission Line. *ApJ* 707, 1334–1346. 0910.2848.
- Warner, C., Hamann, F., Dietrich, M., 2004. Active Galactic Nucleus Emission-Line Properties Versus the Eddington Ratio. *ApJ* 608, 136–148. [arXiv:astro-ph/0402471](#).
- Willott, C.J., Delorme, P., Reyl  , C., Albert, L., Bergeron, J., Crampton, D., Delfosse, X., Forveille, T., Hutchings, J.B., McLure, R.J., Omont, A., Schade, D., 2010. The Canada-France High- $z$  Quasar Survey: Nine New Quasars and the Luminosity Function at Redshift 6. *AJ* 139, 906–918. 0912.0281.
- Wills, B.J., Brotherton, M.S., Fang, D., Steidel, C.C., Sargent, W.L.W., 1993. Statistics of QSO Broad Emission-Line Profiles. I. The C IV  $\lambda$ 1549 Line and the  $\lambda$ 1400 Feature. *ApJ* 415, 563–+.
- Wills, B.J., Browne, I.W.A., 1986. Relativistic beaming and quasar emission lines. *ApJ* 302, 56–63.
- Woo, J.H., Treu, T., Barth, A.J., Wright, S.A., Walsh, J.L., Bentz, M.C., Martini, P., Bennert, V.N., Canalizo, G., Filippenko, A.V., Gates, E., Greene, J., Li, W., Malkan, M.A., Stern, D., Minezaki, T., 2010. The Lick AGN Monitoring Project: The  $M_{\text{BH}}\text{-}\sigma_*$  Relation for Reverberation-mapped Active Galaxies. *ApJ* 716, 269–280. 1004.0252.
- Zamanov, R., Marziani, P., Sulentic, J.W., Calvani, M., Dultzin-Hacyan, D., Bachev, R., 2002. Kinematic Linkage between the Broad- and Narrow-Line-emitting Gas in Active Galactic Nuclei. *ApJL* 576, L9–L13. [arXiv:astro-ph/0207387](#).
- Zamfir, S., Sulentic, J.W., Marziani, P., 2008. New insights on the QSO radio-loud/radio-quiet dichotomy: SDSS spectra in the context of the 4D eigenvector1 parameter space. *MNRAS* 387, 856–870. 0804.0788.
- Zamfir, S., Sulentic, J.W., Marziani, P., Dultzin, D., 2010. Detailed characterization of H $\beta$  emission line profile in low- $z$  SDSS quasars. *MNRAS* 403, 1759. 0912.4306.

- Zel'Dovich, Y.B., Novikov, I.D., 1965. Mass of Quasi-Stellar Objects. *Soviet Physics Doklady* 9, 834–+.
- Zhou, H., Wang, T., Yuan, W., Lu, H., Dong, X., Wang, J., Lu, Y., 2006. A Comprehensive Study of 2000 Narrow Line Seyfert 1 Galaxies from the Sloan Digital Sky Survey. I. The Sample. *ApJS* 166, 128–153. [arXiv:astro-ph/0603759](#).
- Zhou, X.L., Zhang, S.N., Wang, D.X., Zhu, L., 2010. Calibrating the Correlation Between Black Hole Mass and X-ray Variability Amplitude: X-ray Only Black Hole Mass Estimates for Active Galactic Nuclei and Ultra-luminous X-ray Sources. *ApJ* 710, 16–23. [0912.2636](#).